

The fragmentation dynamics of simple organic molecules of astrochemical interest interacting with VUV photons

Stefano Falcinelli, Franco Vecchiocattivi, Fernando Pirani, Michele Alagia, Luca Schio, Robert Richter, Stefano Stranges, Vitali Zhaunerchyk, Nadia Balucani, and Marzio Rosi

ACS Earth Space Chem., **Just Accepted Manuscript** • DOI: 10.1021/
acsearthspacechem.9b00115 • Publication Date (Web): 12 Aug 2019

Downloaded from pubs.acs.org on August 12, 2019

Just Accepted

“Just Accepted” manuscripts have been peer-reviewed and accepted for publication. They are posted online prior to technical editing, formatting for publication and author proofing. The American Chemical Society provides “Just Accepted” as a service to the research community to expedite the dissemination of scientific material as soon as possible after acceptance. “Just Accepted” manuscripts appear in full in PDF format accompanied by an HTML abstract. “Just Accepted” manuscripts have been fully peer reviewed, but should not be considered the official version of record. They are citable by the Digital Object Identifier (DOI®). “Just Accepted” is an optional service offered to authors. Therefore, the “Just Accepted” Web site may not include all articles that will be published in the journal. After a manuscript is technically edited and formatted, it will be removed from the “Just Accepted” Web site and published as an ASAP article. Note that technical editing may introduce minor changes to the manuscript text and/or graphics which could affect content, and all legal disclaimers and ethical guidelines that apply to the journal pertain. ACS cannot be held responsible for errors or consequences arising from the use of information contained in these “Just Accepted” manuscripts.

1
2
3
4
5
6
7 The fragmentation dynamics of simple organic
8
9
10
11 molecules of astrochemical interest interacting with
12
13
14
15 VUV photons
16
17
18
19

20 *Stefano Falcinelli,*¹ Franco Vecchiocattivi,¹ Fernando Pirani,² Michele Alagia,³ Luca Schio,³*
21
22 *Robert Richter,⁴ Stefano Stranges,⁵ Vitali Zhaunerchyk,⁶ Nadia Balucani,² and Marzio Rosi^{1,7}*
23
24
25

26 ¹Department of Civil and Environmental Engineering, University of Perugia, Via G. Duranti 93,
27
28 06125 Perugia, Italy
29
30

31 ²Department of Chemistry, Biology and Biotechnologies, University of Perugia, Via Elce di
32
33 Sotto 8, 06123 Perugia, Italy
34
35
36

37 ³IOM CNR Laboratorio TASC, 34012 Trieste, Italy
38
39

40 ⁴Sincrotrone Trieste, Area Science Park, 34149, Basovizza, Trieste, Italy
41
42

43 ⁵Department of Chemistry and Drug Technology, University of Rome Sapienza, 00185 Rome,
44
45 Italy
46
47
48

49 ⁶Department of Physics, University of Gothenburg, Gothenburg, 412 96, Sweden
50
51

52 ⁷ISTM-CNR, 06123 Perugia, Italy
53
54
55
56
57
58
59
60

1
2
3 KEYWORDS: Propylene oxide, N-methylformamide, double photoionization, synchrotron
4
5 radiation, molecular dication, Coulomb explosion, electron-ion-ion coincidence, astrochemistry.
6
7
8
9

10
11
12
13 ABSTRACT: An experimental investigation on the fragmentation dynamics following the double
14
15 photoionization of simple organic molecules of astrochemical interest, propylene oxide and N-
16
17 methylformamide molecules, induced by VUV photons has been reported. Experiments used
18
19 linearly polarized light in the 18-37 eV (propylene oxide) and 26-45 eV (N-methylformamide)
20
21 photon energy range at the ELETTRA Synchrotron Facility of Trieste (Italy), coupling ion imaging
22
23 and electron-ion-ion coincidence techniques with time-of-flight mass spectrometry. In the case of
24
25 propylene oxide, six different two-body fragmentation processes have been recorded with the
26
27 formation of $\text{CH}_2^+/\text{C}_2\text{H}_4\text{O}^+$, $\text{CH}_3^+/\text{C}_2\text{H}_3\text{O}^+$, $\text{O}^+/\text{C}_3\text{H}_6^+$, $\text{OH}^+/\text{C}_3\text{H}_5^+$, $\text{C}_2\text{H}_3^+/\text{CH}_3\text{O}^+$, $\text{C}_2\text{H}_4^+/\text{CH}_2\text{O}^+$
28
29 ion pairs. On the other hand, the double photoionization of N-methylformamide occurs producing
30
31 two main fragmentation reactions, forming $\text{CH}_3^+ + \text{CH}_2\text{NO}^+$ and $\text{H}^+ + \text{C}_2\text{H}_4\text{NO}^+$. The relative cross
32
33 sections and the threshold energies for all fragmentation channels are recorded as a function of the
34
35 photon energy. Furthermore, in the case of the double photoionization of propylene oxide, the
36
37 measure of the kinetic energy released distribution for the $\text{CH}_3^+/\text{C}_2\text{H}_3\text{O}^+$ final ions with their
38
39 angular distributions allowed the identification of a bimodal behavior indicating the possible
40
41 formation of two different stable isomers of $\text{C}_2\text{H}_3\text{O}^+$: acetyl and oxiranyl cations. The obtained
42
43 results are important to clarify the physical chemistry of the elementary processes induced by the
44
45 interaction of ionizing radiations with simple organic molecules of astrochemical interest:
46
47 propylene oxide and N-methylformamide.
48
49
50
51
52
53
54
55
56
57
58
59
60

I. INTRODUCTION

After the first detection in space of CH and CN as well as of CH⁺ ions¹, more than a hundred molecules and dozens of ions (both cationic and anionic species) have been discovered in interstellar and circumstellar environments whose list is constantly updated.^{2,3} Nowadays it is believed that ion-molecule reactions are very important in the evolution process of interstellar clouds, where chemical reactions between neutral species are hindered by the critical physical conditions characterizing these environments: very low density ($0.1-10^4$ particles/cm³, at least a factor 10^{15} lower than the terrestrial atmosphere) and temperature (10-100 K).³ In fact, unlike neutral-neutral chemical reactions, in general characterized by the presence of an activation energy, ion-molecules reactions are barrierless processes and this is consistent with proposed chemical models of interstellar cloud evolution where dissociative recombination induced by free electrons appears to be the final process responsible for the neutralization of ions into neutral species.¹ Since the solar systems come from interstellar clouds, the chemistry of the latter is of particular relevance for understanding the chemical composition developed in planets and comets. Consequently, the chemical species in the interstellar clouds can be considered as the basic building blocks for the synthesis of increasingly complex molecules that were responsible for the emergence of life on our planet.⁴⁻⁶

It is well known that ionic species can be produced in space by cosmic rays (protons, α particles, electrons, γ -rays, and heavier nuclei such as C⁶⁺ with a large energy content up to 100 GeV), UV and extreme-UV photons, X-rays, shock waves, whose relative importance in ionization processes depends on the peculiarity of the involved extraterrestrial environment.⁷ Among the sources of ionizing radiations active in space, it is interesting to note the presence of synchrotron radiation. It is naturally produced at low frequency in the magnetic fields, for example enveloping Earth and

1
2
3 Jupiter, whereas some of the most spectacular ultra-relativistic sources of this type of radiation are
4 outside the Solar System. Among these, the best known is the Crab Nebula, where the synchrotron
5 emission ranges from blue to ultraviolet.⁸ The presence of ionizing radiation in space is responsible
6 also for the formation of doubly charged species, commonly called atomic or molecular dications.
7 These species have been detected in comet tails and in the upper planetary atmospheres^{9,10} where
8 they can play an important role, as well as in the envelope of young stellar objects.¹¹ In particular,
9 recent studies indicate the possible important role of CO_2^{2+} molecular dications in the continuous
10 erosion of the Mars atmosphere. They proposed an explanation of the anomalous O^+ density profile
11 recorded by Viking lander and Mariner 6 spacecraft.¹²⁻¹⁴ In fact, the atmosphere of Mars is very
12 rich in CO_2 that can be double ionized with the formation of CO_2^{2+} dications. This species is
13 metastable and dissociates by Coulomb explosion with subsequent formation of CO^+ and O^+ ions
14 having a very high kinetic energy content. In particular, O^+ ions are formed with a translational
15 energy content of about 3.8 eV, large enough to allow their escape from the upper atmosphere of
16 Mars into space.^{13,14}

17
18
19 In this paper, we present recent results obtained in the study of fragmentation processes induced
20 by the interaction of ionizing vacuum ultraviolet VUV photons with organic molecules of
21 relevance in astrochemistry: i) propylene oxide being the first chiral molecule detected by
22 astronomers using highly sensitive radio telescopes in interstellar space;¹⁵ ii) N-methylformamide,
23 which is one of the simplest organic molecules containing the peptide bond, recently discovered
24 in interstellar medium¹⁶ and of particular interest in order to investigate its selective fragmentation
25 induced by UV photons.

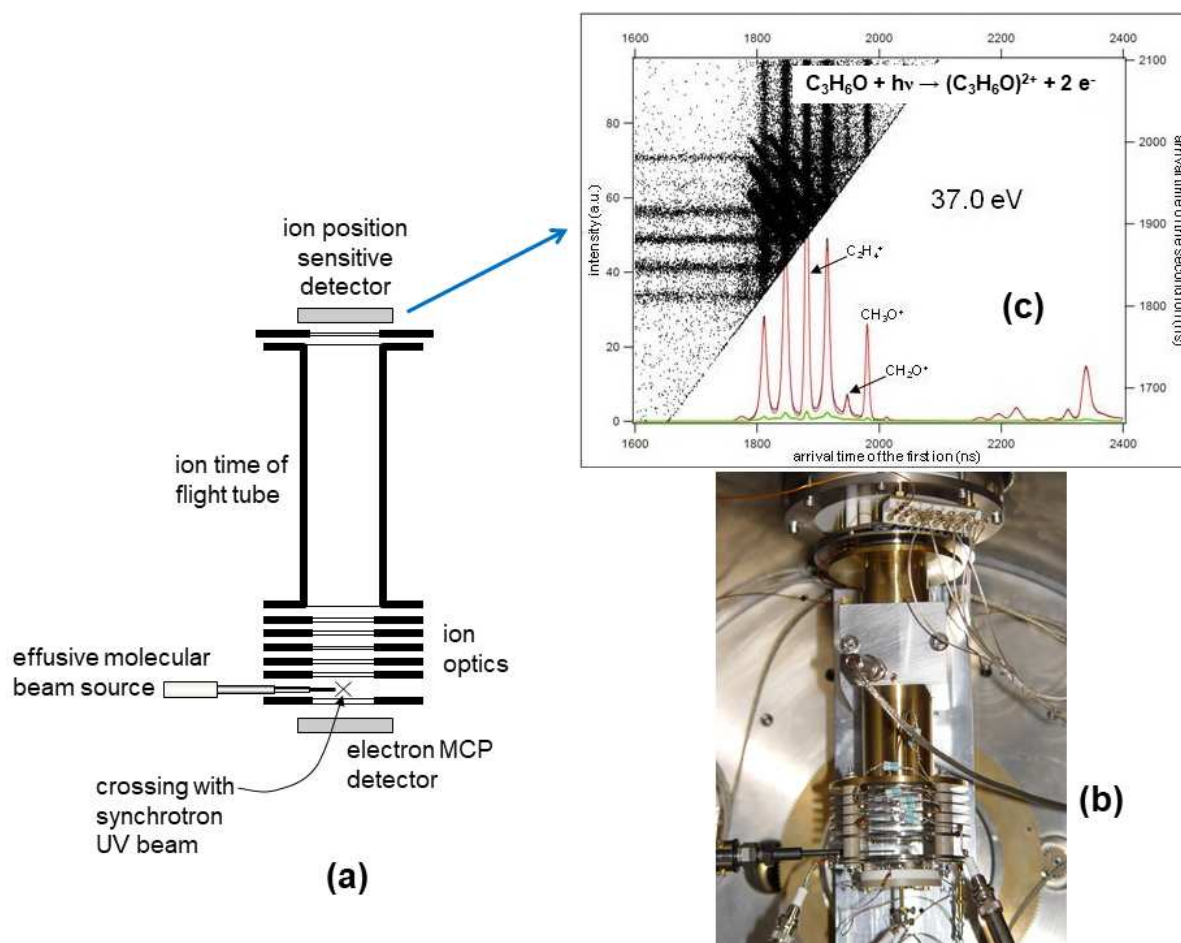
26
27
28 To investigate the interaction between such molecular systems and ionizing VUV radiation we
29 performed preliminary experiments using linearly polarized synchrotron radiation at the

1
2
3 “Circular Polarization (CiPo)” Beamline of ELETTRA Synchrotron Facility (Trieste, Italy):
4
5 double photoionization studies have been carried out employing the ARPES (Angle Resolved
6
7 Photo-Emission Spectroscopy) apparatus successfully used in previous experiments by our
8
9 research group, since almost twenty years.¹⁷⁻¹⁹ More recently, preliminary double
10
11 photoionization of propylene oxide in a racemic mixture, has been carried out in the photon-
12
13 energy range of 18-37 eV, measuring threshold energies for different two-body fragmentation
14
15 processes with their relative cross sections, and the kinetic energy released (KER) distribution of
16
17 fragment ions at different photon energies.^{20,21} In particular, the measure of the KER distribution
18
19 for the $\text{CH}_3^+/\text{C}_2\text{H}_3\text{O}^+$ final ions with their angular distributions allowed the identification of a
20
21 bimodal behavior. In the present paper, we discuss the KER data together with new results
22
23 concerning the recorded $\text{CH}_3^+/\text{C}_2\text{H}_3\text{O}^+$ angular distributions, invoking the presence of two
24
25 different microscopic mechanisms in the dissociation dynamics following the Coulomb
26
27 explosion of the $(\text{C}_3\text{H}_6\text{O})^{2+}$ propylene oxide dication, which is able to form two different stable
28
29 isomers of $\text{C}_2\text{H}_3\text{O}^+$: acetyl and oxiranyl cations (see Section III).
30
31
32
33
34
35

36 On the other hand, N-methylformamide is a relevant simple organic species of great
37
38 astrochemical interest, since it was recently discovered in the interstellar medium, as we have
39
40 already mentioned, and because it is a prototype molecule containing the peptide bond, which is
41
42 so important for life. The data reported here could be of interest in order to clarify if a selective
43
44 cleavage of the peptide bond can be induced by UV photons. This work aims to bring together an
45
46 experimental and theoretical effort, with complementary skills encompassing several fields of
47
48 gas-phase chemistry, like-mass spectrometry, spectroscopy, reaction dynamics, and theoretical
49
50 chemistry.²²⁻²⁴
51
52
53
54
55
56
57
58
59
60

II. EXPERIMENTAL SECTION

Experiments whose data are presented in this paper have been done at the ELETTRA Synchrotron Facility of Basovizza, Trieste (Italy) employing the ARPES end station: the double photoionization of propylene oxide was performed at the “Circular Polarization (CiPo)” beamline, whereas the analogous experiment involving N-methylformamide was done at the “GasPhase” beamline. The 3D-ion-imaging TOF spectrometer (see the schematic and picture presented in Fig. 1a and b, respectively), already used in previous experiments concerning the double dissociative photoionization of N_2O ,^{17,25} CO_2 ,^{26,27} C_6H_6 ,^{28,29} and C_2H_2 ,^{30,31} was utilized.



1
2
3 **Figure 1.** (a) A schematic of the photoelectron-photoion-photoion coincidence (PEPIPICO)
4 device employed in the 3D-ion-imaging time of flight mass spectrometry measurements: the
5 detectors used are micro-channel-plates (MCP) detectors; (b) A picture of the PEPIPICO
6 prototype apparatus; (c) The coincidence spectrum with the relative mass spectrum recorded in
7 the double photoionization experiment of propylene oxide at a photon energy of 37 eV. In this
8 kind of plot, any point corresponds to two time-of-flight values of a pair of ions produced in the
9 same photoionization event and detected in coincidence with ejected photoelectrons from the
10 ionized molecule.
11
12
13
14
15
16
17
18
19
20
21
22
23
24
25

26 Such a tool is a photoelectron-photoion-photoion coincidence (PEPIPICO) instrument, composed
27 of a time-of-flight (TOF) mass spectrometer coupled with an ion-position sensitive detector. This
28 charged-particles detector is a stack of three micro-channel-plates with a multi-anode array
29 arranged in 32 rows and 32 columns and was properly conceived by M. Lavollée³² to allow the
30 measurement of the spatial momentum components of the fragment ion products (see Fig. 1).
31 The signal of a pair of fragment ions, produced by the same double photoionization event and
32 detected in temporal coincidence with the ejected photoelectrons from the neutral molecular
33 precursor, was recorded using the method already employed, where the data analysis has been
34 performed using a properly tested computational procedure,²⁴⁻³¹ whose only main features are
35 given below. Fig. 1c shows a standard coincidence spectrum obtained by the PEPIPICO device
36 described above (see Fig. 1a and b) in the double photoionization of propylene oxide at a photon
37 energy of 37 eV, where the mass spectrum of ions produced by the Coulomb explosion of
38 $C_3H_6O^{2+}$ dication is also reported. In this coincidence plot, any point in the diagonal black traces
39 correlates with two t_1 and t_2 delay TOF values of a pair of ions produced in the same
40
41
42
43
44
45
46
47
48
49
50
51
52
53
54
55
56
57
58
59
60

1
2
3 photoionization event, and measured with respect to the same ejected photoelectron. Product ions
4
5 recorded both in single and double ionization of the neutral molecular precursor are evident in
6
7 the mass spectrum of Fig. 1c together with some background peaks. A careful analysis of
8
9 coincidence spectra recorded at each investigated photon energy (as the one reported in Fig. 1c)
10
11 is able to provide: (i) the relative cross section for all investigated dissociation channels,
12
13 evaluating the density of coincidences in the recorded experimental plots as the one of Fig. 1c;
14
15 (ii) the KER of ionic fragments by a simple analysis based on the methodology proposed by
16
17 Lundqvist *et al.*;³³ (iii) the lifetime of the intermediate molecular dication (produced by double
18
19 ionization of the neutral molecular precursor) by the procedure developed by Field and Eland,³⁴
20
21 analyzing coincidence dot distributions as a function of the arrival time differences (t_2-t_1) of the
22
23 fragment ions to the ion-position-sensitive detector of the PEPICO device. By a Monte Carlo
24
25 trajectory simulation whose details can be found in previous papers,^{35,36} we improved a specific
26
27 computational procedure based on the computation of experimental distribution of the
28
29 coincidences dot density, adjusting the KER and determining the standard deviation as a
30
31 reliability level of the simulation.³⁶
32
33
34
35
36
37

38
39 In our apparatus of Fig. 1, the tunable synchrotron light beam crosses at a right angle to an
40
41 effusive molecular beam of the neutral precursor molecule generated by a stainless-steel needle
42
43 nozzle having a 1.0 mm of diameter. The product ions are collected in coincidence with
44
45 photoelectrons ejected from the same single double photoionization event under study.
46
47

48 Molecular beams of either propylene oxide or N-methylformamide were generated by effusion
49
50 from glass bottles containing commercial samples (with a 99% nominal purity), being provided
51
52 by the needle effusive beam source exploiting their considerable vapor pressure at room
53
54 temperature. In order to satisfy security health standard procedures, a closed system with a
55
56
57
58
59
60

1
2
3 forced ventilation hood was used. At the “CiPo” beamline, during the double photoionization
4 experiment of propylene oxide, a Normal Incidence Monochromator (NIM) was used, equipped
5 with two different holographic gratings: the 18–37 eV energy range was covered by means of a
6 Gold (2400 l/mm) and an Aluminum (1200 l/mm) coated grating. The use of the NIM geometry
7 allowed the reduction of spurious effects due to ionization by photons from higher orders of
8 diffraction. On the other hand, in the double photoionization of N-methylformamide performed
9 at the “GasPhase” beamline (26–45 eV photon energy range), a monochromator using a 400
10 l/mm spherical grating in first diffraction order was employed. Furthermore, a magnesium film
11 filter was placed in the synchrotron radiation beam path avoiding spurious effects due to
12 ionization events generated by photons from higher orders of diffraction. In the two performed
13 experiments the photon energy resolution was of about 1.5–2.0 meV.
14
15
16
17
18
19
20
21
22
23
24
25
26
27
28
29
30
31
32

33 III. RESULTS AND DISCUSSION

34
35

36 The VUV (vacuum ultraviolet) ionizing radiation of simple organic molecules is of relevance for
37 astrochemistry studies since its presence in space, together with extreme ultraviolet (EUV)
38 photons and cosmic rays, appears to be responsible for the limited growth of organic molecules.
39
40 In this section we report on data obtained by VUV and EUV double photoionization of two
41 important organic molecules recently discovered in space: propylene oxide, being the first chiral
42 molecule detected in interstellar cloud Sagittarius B2,¹⁵ and N-methylformamide, an important
43 simple prototype molecule containing the peptide bond recently identified in interstellar
44 medium.¹⁶ Experimental data are presented and discussed in the next two subsections below and
45 concern relative cross sections for each recorded dissociation channel with the relative appearing
46
47
48
49
50
51
52
53
54
55
56
57
58
59
60

1
2
3 threshold energy, the KER distributions for any pairs of product ions, and their final angular
4
5 distribution. Such data are of relevance in order to clarify the microscopic dynamics of the
6
7 fragmentation reactions following the Coulomb explosion of the intermediate $C_3H_6O^{2+}$ and
8
9 $C_2H_5NO^{2+}$ dications formed in the double photoionization of the neutral molecular precursors.
10
11

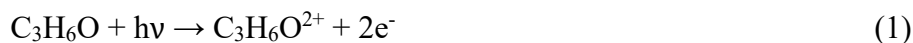
12
13 A full characterization of ionic species (either single- or multiple-charged) generated by ionizing
14
15 radiations in space should consider the role of anisotropy, strength of intermolecular
16
17 interactions^{37,38} as well as stereo-dynamical effects.³⁹ These issues are among the most important
18
19 open queries that need to be clarified in order to entirely outline elementary chemical and
20
21 physical phenomena and evaluate their role in extraterrestrial environments.
22
23

24
25 It should be noted that the analysis of collected coincidence spectra, applying the methodology
26
27 discussed in section II, allowed us to exclude the formation of stable $C_3H_6O^{2+}$ and $C_2H_5NO^{2+}$
28
29 molecular dications in the double photoionization of either propylene oxide or N-
30
31 methylformamide in the 18-37 and 26-45 eV photon energy ranges, respectively. In fact, all
32
33 experimental coincidence spectra indicated a lifetime shorter than ~ 50 ns for both $C_3H_6O^{2+}$ and
34
35 $C_2H_5NO^{2+}$, due to the time limit of the characteristic time window of our electron-ion-ion
36
37 coincidence apparatus.³⁶
38
39
40
41
42

43 **III.1 The fragmentation dynamics of propylene oxide by VUV ionizing radiation.**

44
45

46 The double photoionization of propylene oxide using VUV photons in the range of 18-37 eV
47
48 induces the formation of an intermediate molecular dication with a very short lifetime, less than
49
50 50 ns, with an energy threshold formation of 28.3 ± 0.1 eV, according to the reaction (1) below:
51
52



1
2
3 Once formed, the short lived $C_3H_6O^{2+}$ dication evolves by means of Coulomb explosion towards
4
5 six possible two-body fragmentation reactions giving rise to the production of the following ion
6
7 pair products with the respective relative abundances and threshold energies: $C_2H_4^+/CH_2O^+$
8
9 (66.70%; $h\nu \geq 28.3$ eV), $CH_2^+/C_2H_4O^+$ (7.84%; $h\nu \geq 28.5$ eV), $CH_3^+/C_2H_3O^+$ (5.00%; $h\nu \geq 29.0$
10
11 eV), $O^+/C_3H_6^+$ (1.59%; $h\nu \geq 29.0$ eV), $C_2H_3^+/CH_3O^+$ (18.70%; $h\nu \geq 29.2$ eV), $OH^+/C_3H_5^+$
12
13 (0.17%; $h\nu \geq 32.1$ eV). For all recorded two-body fragmentation channels, the relative cross
14
15 sections have been measured and already published in a previous paper.²⁰
16
17
18
19

20 Looking at the microscopic mechanism according to which the previously mentioned two-body
21
22 fragmentation reactions occur, we can note that the two channels leading to $C_2H_3^+/CH_3O^+$ and
23
24 $OH^+/C_3H_5^+$ ion pairs involved a hydrogen migration inside the intermediate $C_3H_6O^{2+}$ dication,
25
26 which appears to be more arduous in the latter case where the H-shift towards the O atom is
27
28 needed. Furthermore, the fragmentation channel forming the $CH_3^+/C_2H_3O^+$ ion pair products
29
30 could involve two different carbon atoms of the precursor molecular $C_3H_6O^{2+}$ dication: in one
31
32 case the carbon atom of the methyl end of the propylene oxide molecule, while in a second case
33
34 there is the possibility of a hydrogen migration from this methyl group to the end carbon atom
35
36 bound to oxygen. The possibility of distinguishing between different microscopic pathways for
37
38 this fragmentation channel led us towards a deeper understanding of this particular dissociation
39
40 process. For this reason, KER distributions for both $CH_3^+/C_2H_3O^+$ ion products were measured as
41
42 a function of the photon energy. The results are shown in Fig. 2, where it is clear that a bimodal
43
44 behavior characterizes the total KER, as it is well evident in the panel of Fig. 2b reporting the
45
46 two total KER distributions recorded at a photon energy of 35 and 37 eV.
47
48
49
50
51
52
53
54
55
56
57
58
59
60

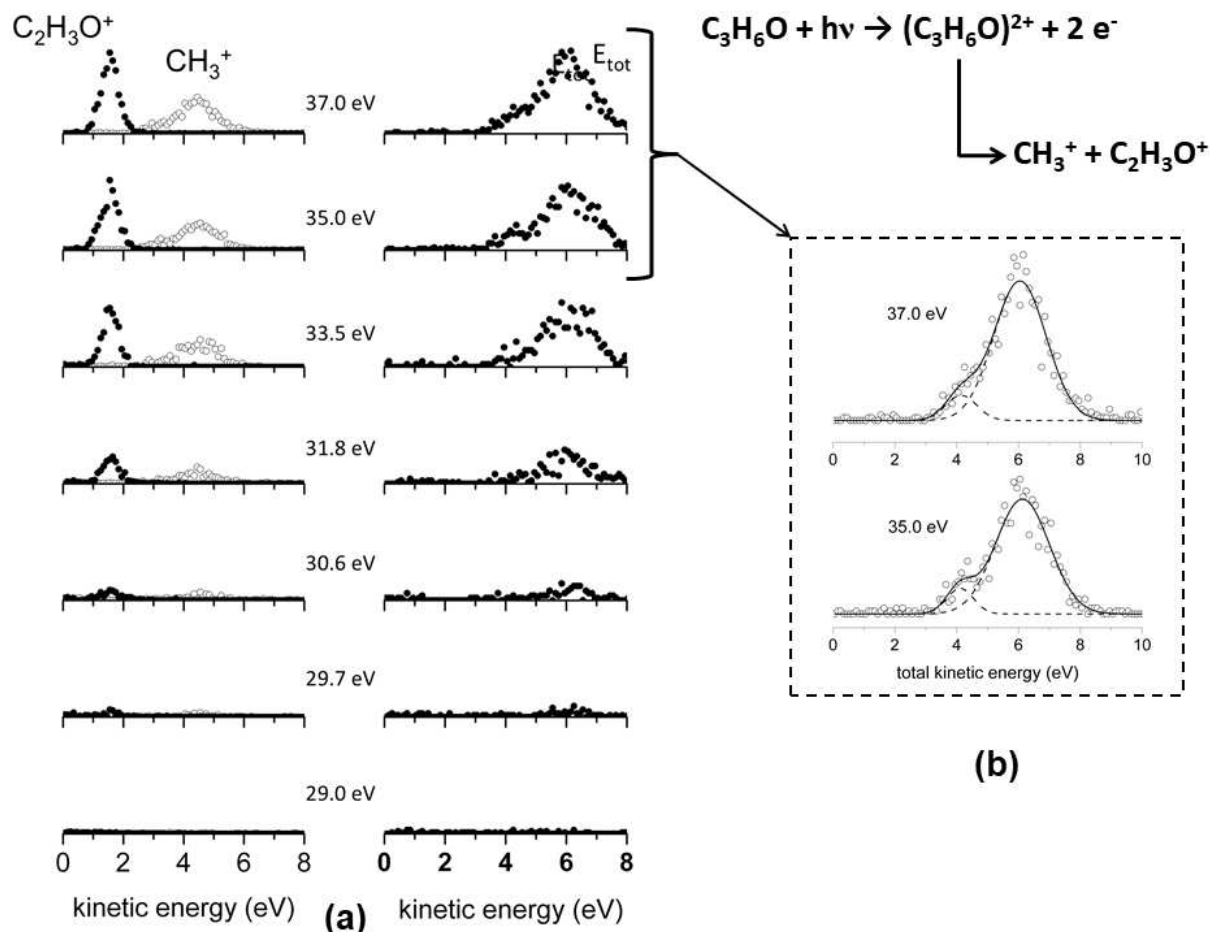
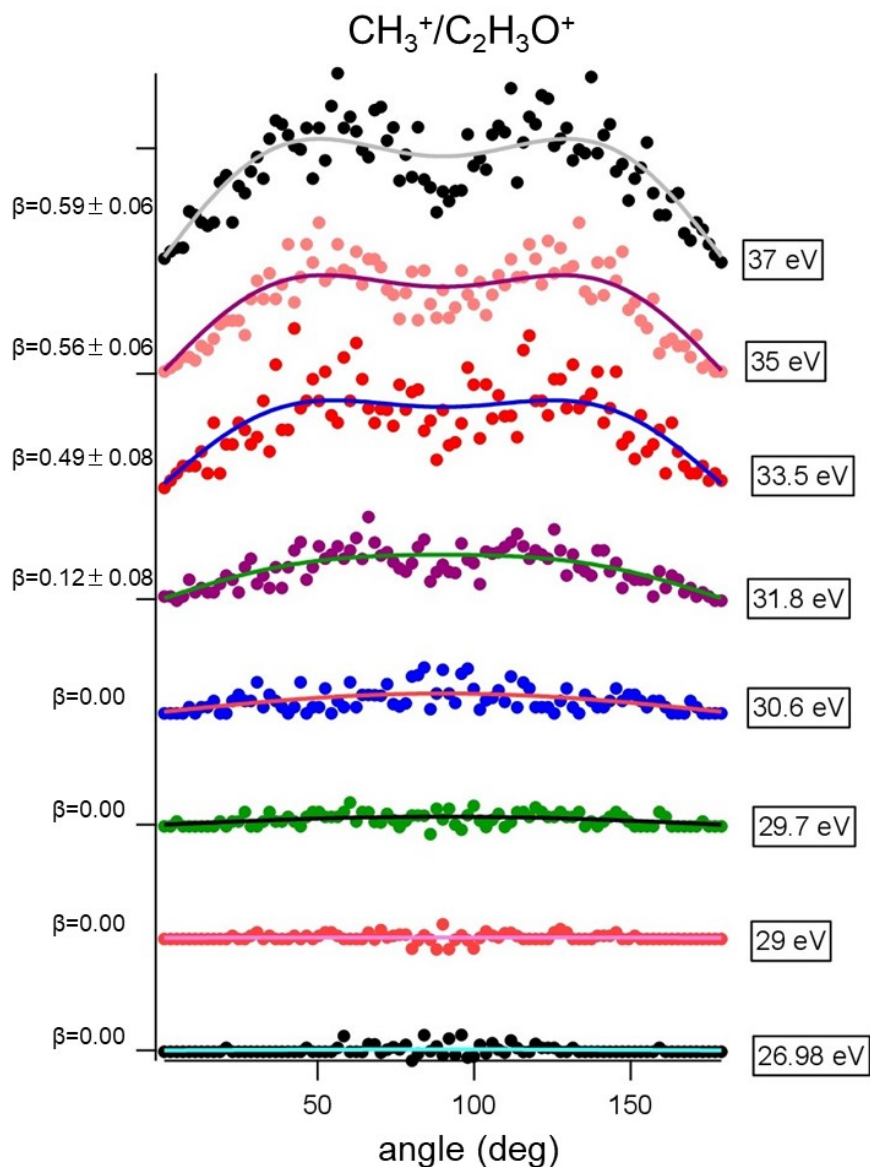


Figure 2. (a) The kinetic energy released (KER) distributions for the $CH_3^+/C_2H_3O^+$ ion pair products generated in the two-body fragmentation process following the double photoionization experiment of propylene oxide as a function of the photon energy: the left panel shows KERs for each single product ion, while in the right panel, total ion KER distributions are reported; (b) Total KER distributions of $CH_3^+/C_2H_3O^+$ ion pairs at a photon energy of 35.0 and 37.0 eV: experimental data (open circles) are the best fitted (full line) using the sum of two different Gaussian functions (dashed lines) pointing out a bimodality behavior due to the existence of two different microscopic reaction mechanisms.

1
2
3 In Fig. 2b, the KER data are best fitted (full line) by a double Gaussian function (dashed line)
4 clearly indicating a bimodal behavior, which is related, as already mentioned above, to the
5 presence of two possible microscopic mechanisms for the two-body fragmentation of $(C_3H_6O)^{2+}$
6 dication producing $CH_3^+ + C_2H_3O^+$. Adopting the methodology described in Section II, the
7 analysis of recorded coincidence spectra at various photon energies allowed us to extract the
8 angular distributions of both $CH_3^+ + C_2H_3O^+$ product ions. Such angular distributions are
9 reported in Fig. 3 at eight different investigated photon energies: two energy values below the
10 threshold energy for such a fragmentation channel (26.98 and 29.0 eV), and six energy values
11 above the threshold (29.7, 30.6, 31.8, 33.5, 35.0, and 37.0 eV). The angular distributions of Fig.
12 3 are 2D images displaying the projection of 3D diffused ion products on the plane of the ion
13 position sensitive micro-channel-plates (MCP) detector (see Fig. 1). The best fit of such 2D maps
14 using the equation (2) below permitted the evaluation of the anisotropy parameter β .⁴⁰⁻⁴²

$$I(\theta) = \frac{\sigma_{tot}}{4\pi} \left[1 + \frac{\beta}{2} (3\cos^2\theta - 1) \right] \quad (2)$$

15
16
17
18
19
20
21
22
23
24
25
26
27
28
29
30
31
32
33
34
35
36 In equation (2), $I(\theta)$ and σ_{tot} stand for the differential and total cross sections of the two-body
37 fragmentation process under study, respectively; θ is the angle between the direction of the light
38 polarization vector and the velocity vector of the recorded fragment ion. The β anisotropy
39 parameter can change in the $-1 \leq \beta \leq 2$ range, depending on the collected distribution of the
40 product ions. The value of $\beta = 0$ is related to an isotropic distribution of ions, while a β value
41 ranging from -1 up to 2 accounts for the emission of product ions that changes slowly from a
42 perpendicular direction with respect to the polarization vector of the light (when is $\beta = -1$), to a
43 parallel direction (with $\beta = 2$).



45
46
47
48
49
50
51
52
53
54
55
56
57
58
59
60

Figure 3. Recorded angular distributions of $\text{CH}_3^+/\text{C}_2\text{H}_3\text{O}^+$ fragment ion pair products formed by Coulomb explosion of the $\text{C}_3\text{H}_6\text{O}^{2+}$ dication at different photon energies. In the ordinate axis, dot intensity is in arbitrary units. For clarity, the error bars are omitted since they are of the same order of magnitude as the dot dimensions. On the left side are reported the calculated anisotropy parameters β using equation (2) for each collected angular distribution (see text).

1
2
3
4
5
6
7 The angular distributions of Fig. 3 appear to be isotropic (with a β value near zero) up to a
8 photon energy of 33.5 eV, where β becomes about 0.49 indicating that an anisotropic component
9 ($\beta > 0.0$), which increases as the photon energy increases, should be considered for a best fitting
10 of the experimental data. This trend could be a confirmation of the possibility that two different
11 microscopic mechanisms are operative for the two-body fragmentation process producing CH_3^+
12 + $\text{C}_2\text{H}_3\text{O}^+$ ions where the bimodal behavior in the KERs distributions of Fig. 2 was found.
13
14
15
16
17
18
19

20 Looking at previous *ab initio* molecular orbital calculations by Nobes *et al.*⁴³, we can propose
21 that by the double photoionization of propylene oxide in the photon energy range of 18-37 eV,
22 different electronic states of the intermediate $\text{C}_3\text{H}_6\text{O}^{2+}$ dication can be formed. Then, by
23 Coulomb explosion, different stable isomers of $\text{C}_2\text{H}_3\text{O}^+$ fragment ions can be produced. In fact,
24 Nobes *et al.* found that two different isomers of $\text{C}_2\text{H}_3\text{O}^+$ can be formed in gas-phase experiments
25 since they are stable.⁴³ They are the most stable acetyl cation [$\text{CH}_3\text{-C=O}$]⁺ (having a linear
26 structure) and the less stable oxiranyl cation [$\text{CH}_2\text{-CH-O}$]⁺ with a cyclic structure characterized
27 by a triangular [$\text{C}\cdots\text{O}\cdots\text{C}$] ring. It should be noted that later Burgers *et al.*⁴⁴ showed the
28 unequivocal identification of both acetyl and oxiranyl $\text{C}_2\text{H}_3\text{O}^+$ isomers in the gas-phase.
29
30
31
32
33
34
35
36
37
38
39
40
41

42 Recently, we carried out CCSD(T)/aug-cc-pVTZ calculations as we have done in previous
43 systems^{6,28,29} with a higher level of accuracy than the data published in 1983 by Nobes *et al.*⁴³
44 confirming that the difference in the energetic stability between the most stable acetyl cation and
45 the two other isomers (oxiranyl and hydroxyvinyl) is not very great. From our calculations, the
46 acetyl cation is about 1.82 eV more stable with respect to the hydroxyvinyl cation. This is in
47 good agreement with previous calculations by Nobes *et al.*,⁴³ who found a value of ≈ 1.87 eV.
48
49 Furthermore, in our case the oxiranyl cation has been found at about 2.39 eV above the acetyl
50
51
52
53
54
55
56
57
58
59
60

one, which is in fairly good agreement with the previous *ab initio* calculations by Nobes *et al.*,⁴³ that fixed the difference in stability between oxiranyl and acetyl cations at ≈ 2.53 eV.

In addition, the B3LYP method^{45,46} has been used to define the optimized geometry for the three stable $C_2H_3O^+$ isomers. Fig. 4 shows the optimized structures of acetyl, hydroxyvinyl, and oxiranyl cations. In the figure, the relative energies, with respect to the most stable isomer, computed both at B3LYP and CCSD(T) level are also reported, and zero-point energy corrections are included. All optimized geometrical structures of Fig. 4, with their relative bond angles and distances, are in good agreement with previous calculations.⁴³

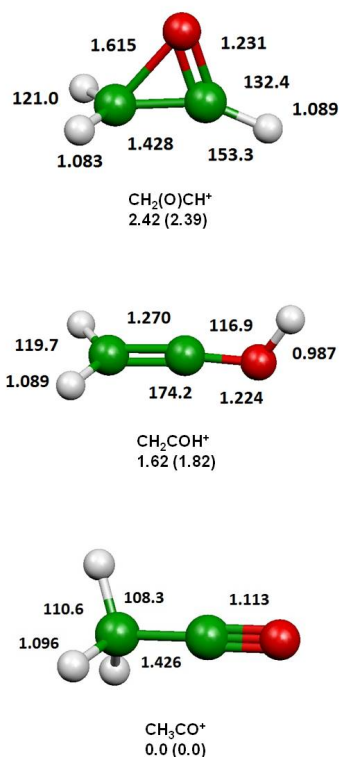


Figure 4. B3LYP optimized geometries (Å, and °) of the three stable $C_2H_3O^+$ isomers; relative energies (eV) computed at B3LYP (CCSD(T)) level have been reported (see text).

1
2
3
4
5
6
7 In Fig. 5 are reported the KER and the angular distributions recorded as a function of the photon
8 energy for the main important two-body dissociation channel producing the $C_2H_4^+/CH_2O^+$ ion
9 pair, having a relative abundance of about 67%. It should be noted that the KER distributions of
10 Fig. 5a are almost the same at each investigated photon energy (29.0, 29.7, 30.6, 31.8, 33.5, 35.0,
11 and 37.0 eV), being rather symmetric. They can be fitted using a simple Gaussian function with
12 peak positions and shapes almost constant with the photon energy. This behavior has been
13 recorded also for the other less abundant two-body fragmentation channels (producing
14 $CH_2^+/C_2H_4O^+$, $O^+/C_3H_6^+$, $C_2H_3^+/CH_6O^+$)²¹ with the only exception of the channel giving rise to
15 the formation of $CH_3^+/C_2H_3O^+$ ion pair whose bimodality has already been discussed above.
16
17
18
19
20
21
22
23
24
25
26
27
28
29
30
31
32
33
34
35
36
37
38
39
40
41
42
43
44
45
46
47
48
49
50
51
52
53
54
55
56
57
58
59
60

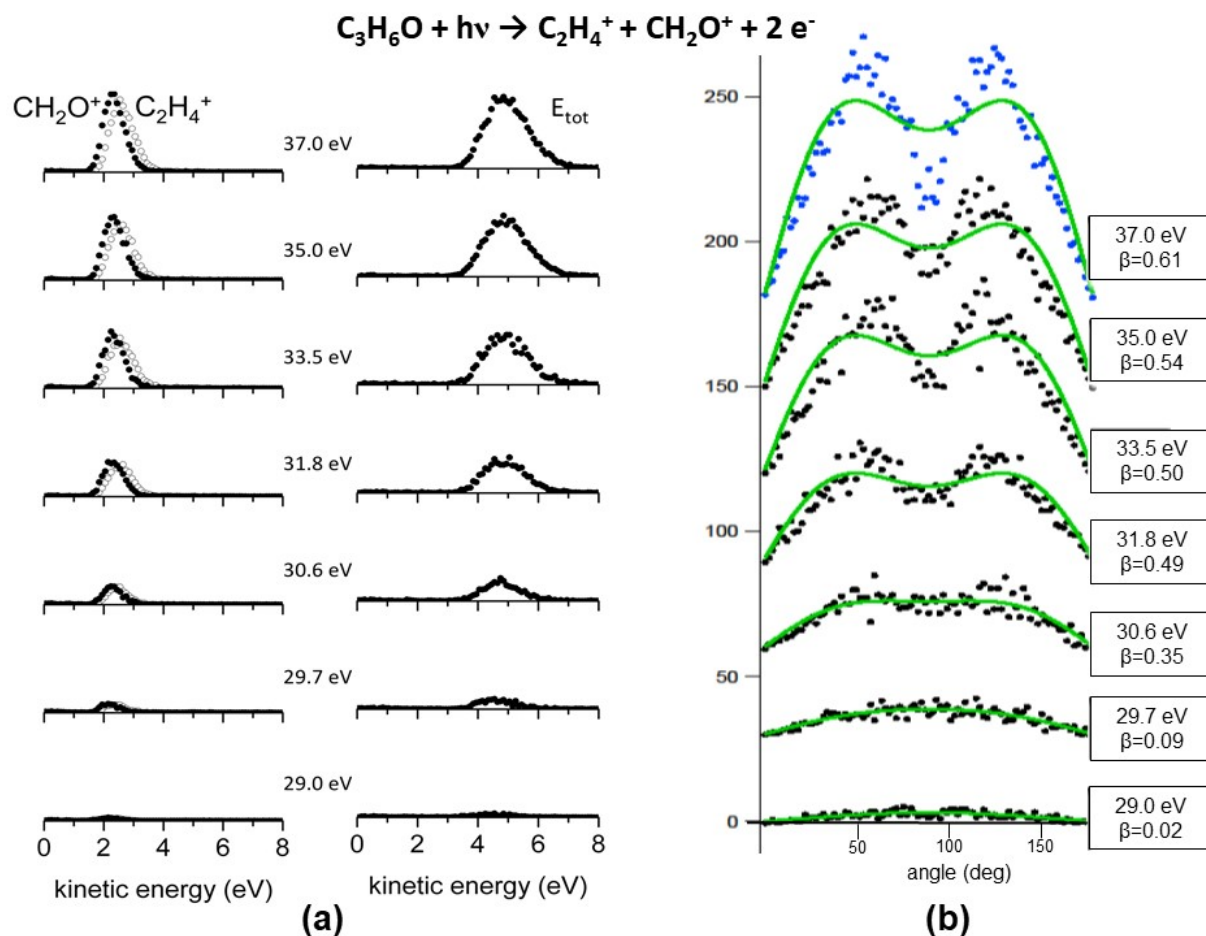


Figure 5. a) The kinetic energy released (KER) distributions for the $\text{C}_2\text{H}_4^+/\text{CH}_2\text{O}^+$ ion pair products generated in the two-body fragmentation process following the double photoionization experiment of propylene oxide as a function of the photon energy: the left panel shows KERs for each single product ion, while in the right panel total ion KER distributions are reported; (b) Angular distributions of $\text{C}_2\text{H}_4^+/\text{CH}_2\text{O}^+$ fragment ion pair products formed by Coulomb explosion of the $\text{C}_3\text{H}_6\text{O}^{2+}$ dication at different photon energies. In the ordinate axis, dot intensity is in arbitrary units. For clarity, the error bars are omitted since they are of the same order of magnitude as the dot dimensions. On the right side are reported the calculated anisotropy parameters β using equation (2) for each collected angular distribution (see text).

1
2
3
4
5
6
7 The similarity of behavior in almost all the recorded KERs could be an evidence that for each
8 dissociation channel just one specific region of the multidimensional potential energy surface
9 (related to the effective intramolecular interaction within the $(\text{C}_3\text{H}_6\text{O})^{2+}$ intermediate molecular
10 dication frame and responsible of the formation of the various two-body fragmentation channels)
11 should be involved. This means that the excess of the employed photon energy with respect to
12 the threshold of the double ionization energy should be released as electron recoil energy for all
13 investigated fragmentation channels with the exception of the one forming $\text{CH}_3^+ + \text{C}_2\text{H}_3\text{O}^+$
14 products. The peculiarity of this fragmentation channel with respect to all the others appears to
15 be confirmed by a comparative analysis of the angular distributions reported in Fig. 3 and Fig.
16 5b. The angular distributions of Fig. 5b, related to the main two-body fragmentation channel
17 producing the $\text{C}_2\text{H}_4^+/\text{CH}_2\text{O}^+$ ion pair, are characterized by a gradual increase of the anisotropy
18 parameter β indicating that $\text{C}_2\text{H}_4^+/\text{CH}_2\text{O}^+$ ions are emitted by the Coulomb explosion of the
19 $(\text{C}_3\text{H}_6\text{O})^{2+}$ dication in a preferential direction that is parallel with respect to the polarization
20 vector of the ionizing used light. On the other hand, as we have already discussed above, the
21 angular distributions of Fig. 3 show a quite sudden change in the β value, passing from an
22 isotropic distribution of the produced $\text{CH}_3^+/\text{C}_2\text{H}_3\text{O}^+$ ion pair ($\beta \approx 0-0.1$), which is maintained up
23 to about 32 eV, to an evident anisotropy (with $\beta \geq 0.5$), which still remains up to 37.0 eV.
24
25
26
27
28
29
30
31
32
33
34
35
36
37
38
39
40
41
42
43
44
45

46 **III.2 The fragmentation dynamics of N-methylformamide by VUV/EUV ionizing radiation.**

47 Preliminary data from a dissociative double photoionization study of N-methylformamide are
48 reported in this section. They concern the relative cross sections for the observed two-body
49
50
51
52
53
54
55
56
57
58
59
60

1
2
3 fragmentation processes coming out of the Coulomb explosion of the intermediate $C_2H_5NO^{2+}$
4
5 dication, with their threshold energies.
6
7

8
9 Previous studies concerning the ionization of N-methylformamide were performed by: i) Lin *et*
10
11 *al.*⁴⁷ with their highly selective dissociation study of the peptide bonds in the N-
12
13 methylformamide and N-methylacetamide, using tunable X-ray photons and investigating the K-
14
15 edge absorption of the atoms connected to the peptide bond; ii) Li *et al.*⁴⁸ who carried out the
16
17 determination of all cation fragments produced by a 70 eV electron ionization with subsequent
18
19 fragmentation of methylated formamides. Later on, Salén *et al.*²³ performed near-edge X-ray
20
21 absorption fine-structure studies for N-methylformamide, N,N-dimethylformamide, and N,N-
22
23 dimethylacetamide, being simple prototypical molecules containing the amide moiety.
24
25
26
27

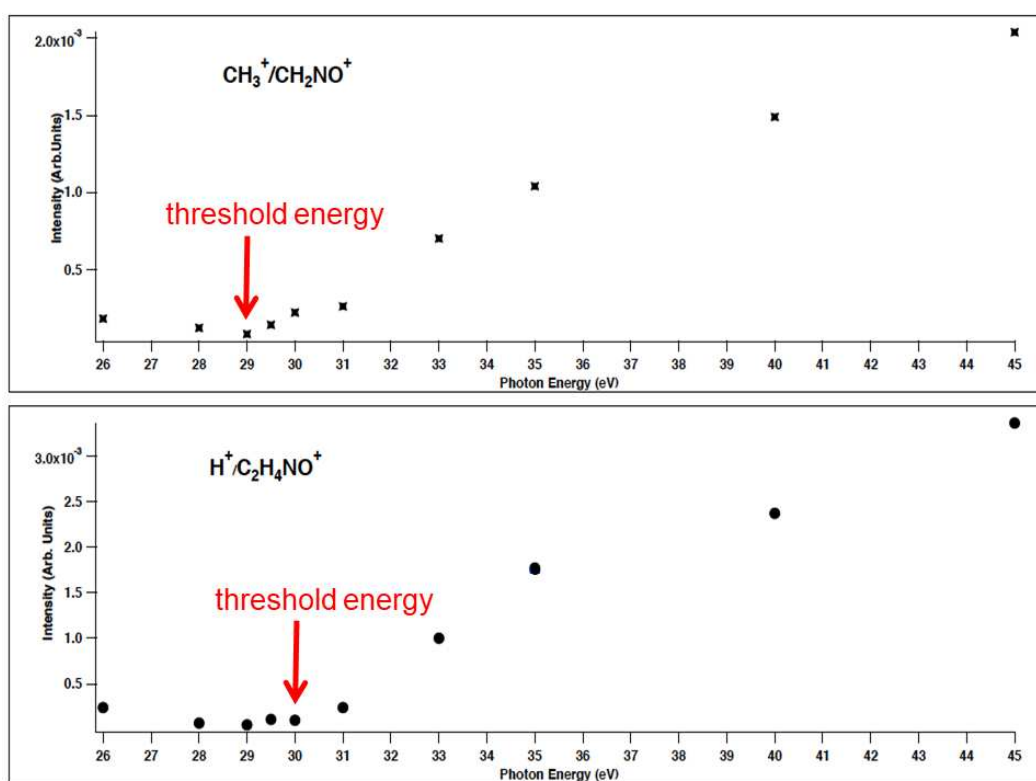
28 The experiment reported here is the first attempt to study the ejection of a pair of valence-shell
29
30 electrons from a simple molecule containing the peptide bond. It was recently performed at the
31
32 “GasPhase” beamline of ELETTRA Synchrotron Facility (Trieste, Italy) using a tunable
33
34 synchrotron radiation in the 26-45 eV photon energy range. The preliminary collected
35
36 coincidence spectra as a function of the photon energy indicate that the following two-body
37
38 dissociation reactions (see equations (3) and (4) below) are operative:
39
40
41
42



45
46
47
48
49 As already mentioned above, no indication for the formation of a stable $C_2H_5NO^{2+}$ molecular
50
51 dication has been found in any recorded mass spectra. In fact, all collected coincidence plots
52
53
54
55
56
57
58
59
60

1
2
3 showed the formation of a short-lived intermediate ($\text{C}_2\text{H}_5\text{NO}^{2+}$)* dication having a lifetime less
4 than 50 ns.
5
6

7
8
9 Applying the procedure discussed in Section II, we were able to determine the relative cross
10 sections for the two observed fragmentation channels (see equations (3) and (4) above) by
11 analyzing the recorded coincidence spectra for each investigated photon energy. Such cross
12 sections are given in Fig. 6 over the probed 26-45 eV photon energy range.
13
14
15
16
17
18



46 **Figure 6.** The relative cross sections as function of the investigated photon energy as obtained in
47 the double photoionization experiment of N-methylformamide in the 26-45 eV photon energy
48 range.
49
50
51
52
53
54
55
56
57
58
59
60

From Fig. 6 it can be seen that the main important two-body fragmentation channel is the one forming $\text{H}^+ + \text{C}_2\text{H}_4\text{NO}^+$ product ions, with about 60% of the relative abundance in the whole investigated photon energy range. Such a channel is characterized by a threshold energy of 30.0 ± 0.3 eV, whereas the other fragmentation channel producing $\text{CH}_3^+ + \text{CH}_2\text{NO}^+$ products is about 40% of the total double photoionization events having a lower threshold energy of 29.0 ± 0.3 eV.

In Figures 7 and 8 are reported the KER distributions (for either total or single fragment ion formation) recorded at two different photon energies (35.0 and 45.0 eV) above the threshold for the two dissociation channels revealed in our experiment.

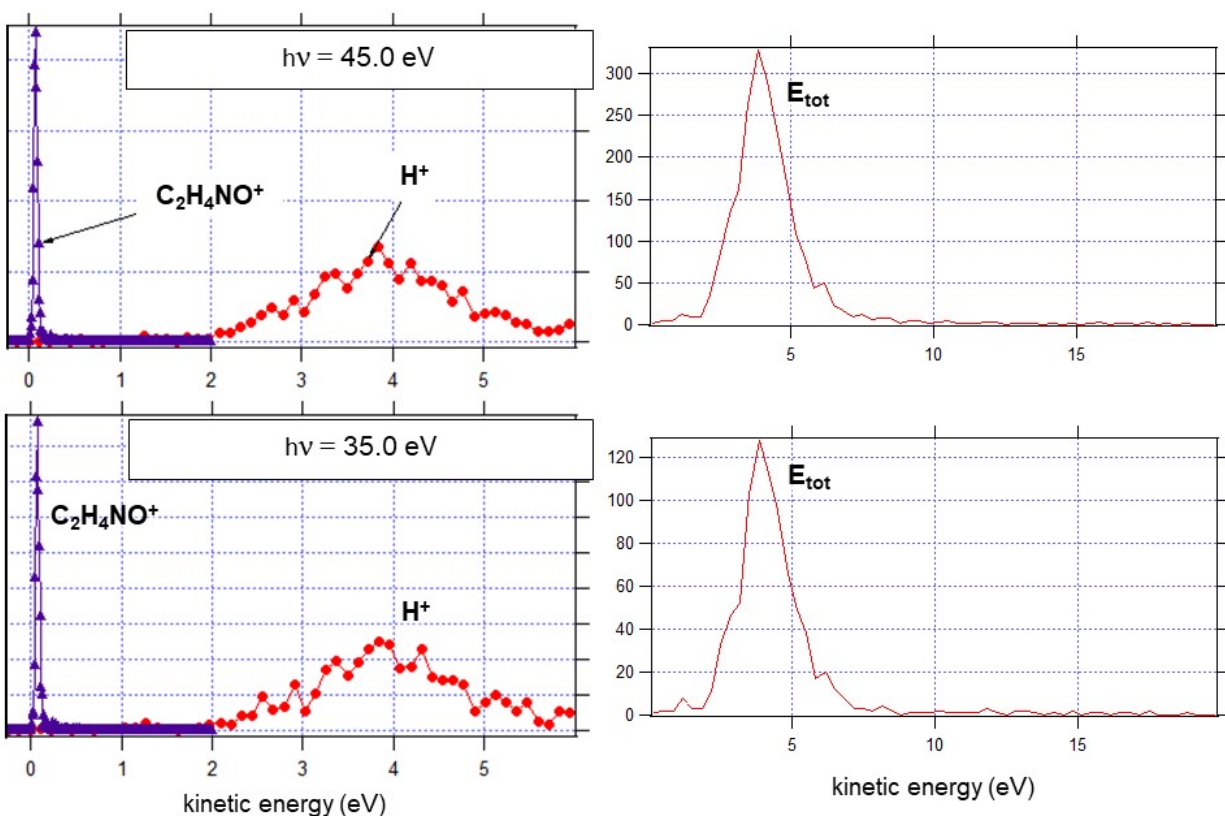
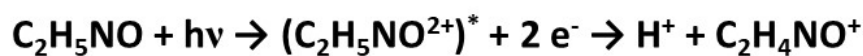


Figure 7. The kinetic energy released (KER) distributions for the $\text{H}^+/\text{C}_2\text{H}_4\text{NO}^+$ ion pair products generated in the two-body fragmentation process following the double photoionization experiment of N-methylformamide at two different photon energies (35.0 eV - lower panel and 45.0 eV – upper panel): the pictures on the left side show KERs for each single product ion, while on the right side, total ion KER distributions are reported.

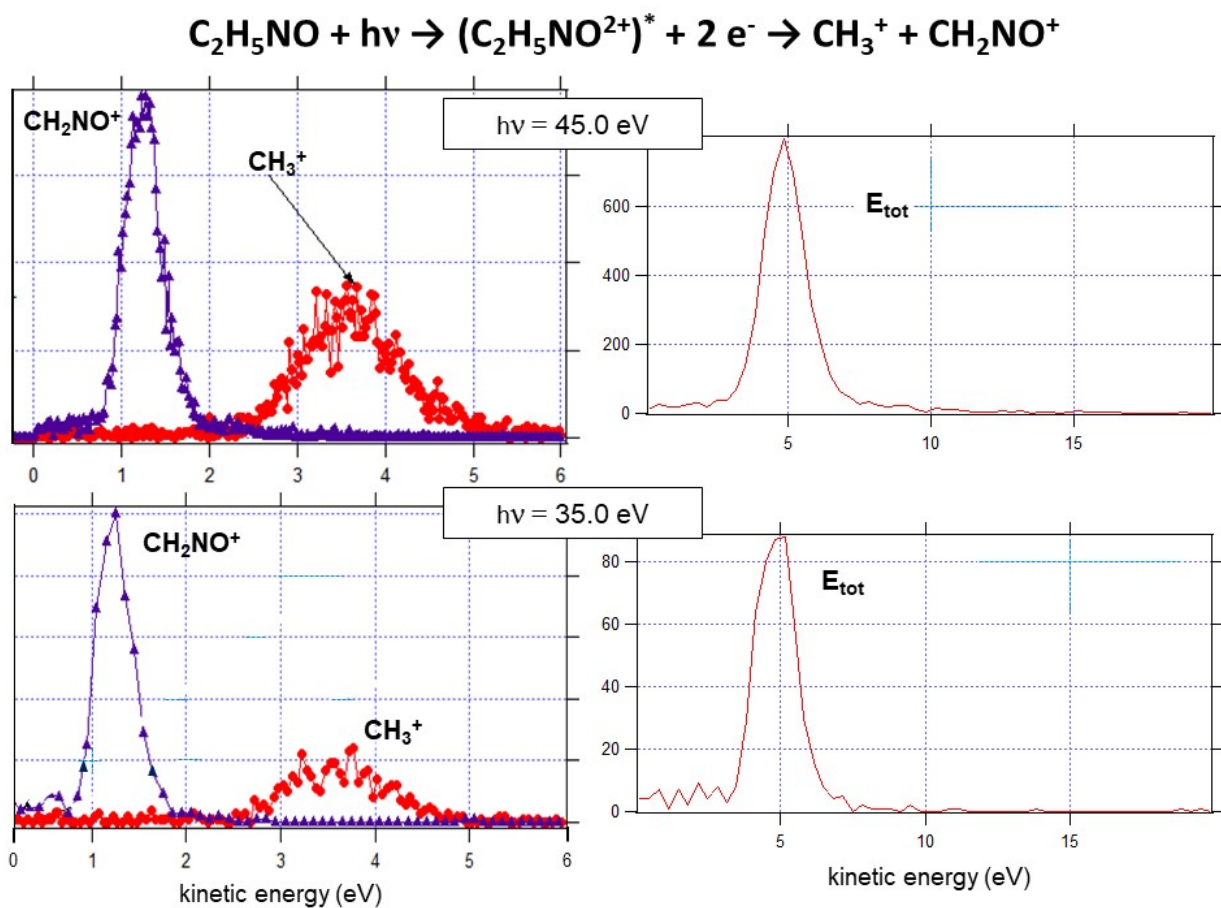


Figure 8. The kinetic energy released (KER) distributions for the $\text{CH}_3^+/\text{CH}_2\text{NO}^+$ ion pair products generated in the two-body fragmentation process following the double photoionization experiment of N-methylformamide at two different photon energies (35.0 eV - lower panel and

1
2
3 45.0 eV – upper panel): the pictures on the left side show KERs for each single product ion,
4
5 while on the right side, total ion KER distributions are reported.
6
7
8
9
10

11
12 In the case of the two-body fragmentation channel leading to $\text{H}^+/\text{C}_2\text{H}_4\text{NO}^+$ ion pair (see equation
13
14 (4)), Fig. 7 (right panel) shows a total KER distribution with a maximum at about 4.0 eV, which
15
16 is found almost completely in the broad distribution of the proton (see left panel of Fig. 7)
17
18 coming out from the Coulomb explosion of the intermediate $(\text{C}_2\text{H}_5\text{NO}^{2+})^*$ molecular dication.
19
20 The second ionic fragment $\text{C}_2\text{H}_4\text{NO}^+$, being much heavier than the other, is characterized by a
21
22 very narrow KER distribution of about 0.2 eV. No differences have been found in the KER
23
24 distributions passing from a photon energy of 35.0 eV up to 45.0 eV. On the other hand, in the
25
26 case of the reaction forming the $\text{CH}_3^+/\text{CH}_2\text{NO}^+$ ion pair (see equation (3)) the total KER
27
28 distributions reported in the right panel of Fig. 8 are almost symmetric and have a maximum at
29
30 about 5.0 eV with a FWHM (Full Width at Half Maximum) of about 1.7 eV.
31
32
33
34
35

36 Furthermore, the KER distributions for single fragment ions reported in the left panel of Fig. 8
37
38 appear to be quite symmetric with a maximum at about 1.3 eV for CH_2NO^+ and ~3.6 eV for
39
40 CH_3^+ , with a broader KER in the latter case because the lighter mass of the methyl fragment (the
41
42 KER of CH_3^+ is characterized by a FWHM of ~1.2 eV compared with a FWHM of ~0.5 eV in
43
44 the case of CH_2NO^+). Moreover, in the case of reaction (3) all recorded KERs shown in Fig. 8 do
45
46 not change as the photon energy changes from 35.0 to 45.0 eV.
47
48
49

50
51 Finally, looking at the typical escape energy of various simple ions,^{13,14} we can argue that the
52
53 measured KER of Figures 7 and 8 for H^+ and CH_3^+ ions (being in the range of 2.2-5.7 eV and
54
55 2.7-4.8 eV, respectively) are compatible with their possible escape from the atmosphere of Mars
56
57
58
59
60

1
2
3 and Titan in the event that N-methylformamide is found to be in these environments in the
4
5 future.
6
7
8
9

10 11 12 IV. CONCLUSIONS 13 14

15 This paper reports on an experimental study concerning the dissociative double photoionization
16 of two simple organic molecules of astrochemical and basic interest, in order to investigate their
17 interaction with UV and EUV ionizing radiations with subsequent direct ejection of two valence
18 electrons. The studied molecules are: i) propylene oxide, being the first chiral molecule recently
19 detected in space;¹⁵ ii) N-methylformamide, being one of the simplest organic molecules
20 containing the peptide bond, discovered in 2017 in interstellar medium¹⁶ and of great interest in
21 order to obtain a deeper understanding of the degradation mechanism of proteins by ionizing
22 radiations.
23
24
25
26
27
28
29
30
31
32

33 Such a study has been performed by using linearly polarized synchrotron radiation in order to
34 identify in each case the leading two-body dissociation channels and to measure: i) the threshold
35 energy for the different ionic products formation; ii) the related branching ratios, and iii) the
36 kinetic energy released distribution of fragment ions at different photon energies. This
37 preliminary study is important in providing new data on $C_3H_6O^{2+}$ and $C_2H_5NO^{2+}$ dication
38 energetics, and nuclear dissociation dynamics, being mandatory information for further
39 experimental and theoretical investigations of the interaction between chiral and peptide bond
40 containing molecules and linearly or circularly polarized light.
41
42
43
44
45
46
47
48
49
50

51 Therefore, we are planning during the next available beamtimes to employ circularly polarized
52 light, as available at the “CiPo” Beamline of ELETTRA Synchrotron Radiation Facility (Trieste,
53
54
55
56
57
58
59
60

Italy), to selectively photo-ionize the two enantiomers of propylene oxide, probing possible differences on the angular and energy distribution of either fragment ions and/or ejected photoelectrons as a function of the radiation energy.

In the case of N-methylformamide, preliminary reported results indicate that UV radiation in the energy range of 26-45 eV is not able to cleave the C-N bond related to the carbonyl functionality. In fact, the equation (3), representing the two-body fragmentation process forming the $\text{CH}_3^+/\text{CH}_2\text{NO}^+$ ion pair, involves the cleavage of one C-N bond of the molecular precursor but it is not the bond to the carbonyl carbon atom. Furthermore, this could be useful for investigations aimed at studying the formation/destruction routes of formamide, which is a well-known abundant simple organic molecule in astrochemical environments.⁴⁹

AUTHOR INFORMATION

Corresponding Author

*Email: stefano.falcinelli@unipg.it – Phone: +39.075.5853862

ORCID - Stefano Falcinelli: 0000-0002-5301-6730

Author Contributions

The manuscript was written through contributions of all authors. All authors have given approval to the final version of the manuscript. All authors contributed equally.

Funding Sources

MIUR (PRIN 2015, STARS in the CAOS- Simulation Tools for Astrochemical Reactivity and Spectroscopy in the Cyber infrastructure for Astrochemical Organic Species, 2015F59J3R).

1
2
3 MIUR and University of Perugia (Italy) within the program “Dipartimenti di Eccellenza 2018-
4 2022”.

5 6 7 8 9 **Notes**

10
11 The authors declare no competing financial interest.

12 13 14 15 **ACKNOWLEDGMENT**

16
17 The scientific staff of CiPo and GasPhase beamlines of the ELETTRA Synchrotron Facility
18 (Trieste, Italy) are gratefully acknowledged. Financial contributions from MIUR (Ministero
19 dell’Istruzione, dell’Università e della Ricerca - PRIN 2015, STARS in the CAOS- Simulation
20 Tools for Astrochemical Reactivity and Spectroscopy in the Cyber infrastructure for
21 Astrochemical Organic Species, 2015F59J3R) is gratefully acknowledged. Support from Italian
22 MIUR and University of Perugia (Italy) is acknowledged within the program “Dipartimenti di
23 Eccellenza 2018-2022”.

24 25 26 27 28 29 30 31 32 33 34 **ABBREVIATIONS**

35
36 UV, ultraviolet; VUV, vacuum ultraviolet; EUV, extreme ultraviolet; PEPIICO, photoelectron-
37 photoion-photoion coincidence; ARPES, angle resolved photoemission spectroscopy; KER,
38 kinetic energy released.

39 40 41 42 43 44 **REFERENCES**

- 45
46 (1) Larsson, M., Geppert, W. D., Nyman, G. Ion chemistry in space. *Rep. Prog. Phys.* **2012**, *75*,
47 066901.
48
49
50
51 (2) Web site: http://www.astrochymist.org/astrochymist_ism.html (accessed online on: July 15th,
52 2019).
53
54
55
56
57
58
59
60

- 1
2
3 (3) Kaiser, R. I. Experimental Investigation on the Formation of Carbon-Bearing Molecules in
4 the Interstellar Medium via Neutral–Neutral Reactions. *Chem. Rev.* **2002**, *102*, 1309–1358.
5
6
7
8
9 (4) Skouteris, D., Balucani, N., Ceccarelli, C., Faginas Lago N., Codella, C., Falcinelli, S., Rosi,
10 M. Interstellar dimethyl ether gas-phase formation: a quantum chemistry and kinetics study.
11 *MNRAS* **2019**, *482*, 3567–3575.
12
13
14
15
16
17 (5) Balucani, N., Skouteris, D., Ceccarelli, C., Codella, C., Falcinelli, S., Rosi, M. A theoretical
18 investigation of the reaction between the amidogen, NH, and the ethyl, C₂H₅, radicals: a possible
19 gas-phase formation route of interstellar and planetary ethanimine. *Mol. Astrophys.* **2018**, *13*, 30-
20 37.
21
22
23
24
25
26
27 (6) Skouteris, D., Balucani, C., Faginas Lago N., Falcinelli, S., Rosi, M. Dimerization of
28 methanimine and its charged species in the atmosphere of Titan and interstellar/cometary ice
29 analogs. *A&A* **2015**, *584*, A76.
30
31
32
33
34
35 (7) Caroff, L. J. and Scargle, J. D. Coherent Synchrotron Emission in the Crab Nebula. *Nature*
36 **1970**, *225*, 168.
37
38
39
40 (8) Alagia, M., Balucani, N., Candori, P., Falcinelli, S., Pirani, F., Richter, R., Rosi, M.,
41 Stranges, S., Vecchiocattivi, F. Production of ions at high energy and its role in extraterrestrial
42 environments. *Rend. Fis. Acc. Lincei* **2013**, *24*, 53–65.
43
44
45
46
47
48 (9) Thissen, R., Witasse, O., Dutuit, O., Wedlund, C. S., Gronoff, G., Lilensten, J. Doubly-
49 charged ions in the planetary ionospheres: a review. *Phys. Chem. Chem. Phys.* **2011**, *13*, 18264-
50 18287.
51
52
53
54
55
56
57
58
59
60

- 1
2
3 (10) Falcinelli, S., Pirani, F., Alagia, M., Schio, L., Richter, R., Stranges, S., Balucani, N.,
4
5 Vecchiocattivi, F. Molecular Dications in Planetary Atmospheric Escape. *Atmosphere* **2016**,
6
7 7(9), 112.
8
9
10
11 (11) Stauber, P., Doty, S. D., van Dishoeck, E. F., Benz, A. O. X-ray chemistry in the envelopes
12
13 around young stellar objects. *A&A* **2005**, 440, 949–966.
14
15
16 (12) Lilensten, J., Wedlund, C. S., Barthélémy, M., Thissen, R., Ehrenreich, D., Gronoff,
17
18 G., Witasse, O. Dications and thermal ions in planetary atmospheric escape. *Icarus* **2013**, 222(1),
19
20 169-187.
21
22
23
24 (13) Falcinelli, S., Pirani, F., Alagia, M., Schio, L., Richter, R., Stranges, S., Vecchiocattivi, F.
25
26 The escape of O⁺ ions from the atmosphere: An explanation of the observed ion density profiles
27
28 on Mars. *Chem. Phys. Lett.* **2016**, 666, 1-6.
29
30
31
32 (14) Falcinelli, S., Rosi, M., Candori, P., Vecchiocattivi, F., Farrar, J. M., Pirani, F., Balucani,
33
34 N., Alagia, M., Richter, R., Stranges, S. Kinetic energy release in molecular dications
35
36 fragmentation after VUV and EUV ionization and escape from planetary atmospheres. *Plan.*
37
38 *Space Sci.* **2014**, 99, 149-157.
39
40
41
42 (15) McGuire, B.A., Carroll, P.B., Loomis, R.A., Finneran, I. A., Jewell, P. R., Remijan A. J.,
43
44 Blake, G. A. Discovery of the interstellar chiral molecule propylene oxide (CH₃CHCH₂O).
45
46 *Science* **2016**, 352, 1449–1452.
47
48
49
50 (16) Belloche, A., Meshcheryakov, A. A., Garrod, R. T., Ilyushin, V. V., Alekseev, E. A.,
51
52 Motiyenko, R. A., Margulès, L., Müller, H. S. P., Menten, K. M. Rotational spectroscopy,
53
54
55
56
57
58
59
60

1
2
3 tentative interstellar detection, and chemical modeling of N-methylformamide. *A&A* **2017**, *601*,
4
5 A49.

6
7
8 (17) Alagia, M., Candori, P., Falcinelli, S., Lavollée, M., Pirani, F., Richter, R., Stranges, S.,
9
10 Vecchiocattivi, F. Anisotropy of the angular distribution of fragment ions in dissociative double
11
12 photoionization of N₂O molecules in the 30-50 eV energy range. *J. Chem. Phys.* **2007**, *126*(20),
13
14 201101.

15
16
17 (18) Alagia, M., Biondini, F., Brunetti, B.G., Candori, P., Falcinelli, S., Teixidor, M.M., Pirani,
18
19 F., Richetr, R., Stranges, S., Vecchiocattivi, F. The double photoionization of HCl: An ion-
20
21 electron coincidence study. *J. Chem. Phys.* **2004**, *121*(21), 10508–10512.

22
23
24 (19) Alagia, M., Boustimi, M., Brunetti, B.G., Candori, P., Falcinelli, S., Richter, R., Stranges,
25
26 S., Vecchiocattivi, F. Mass Spectrometric Study of Double Photoionization of HBr Molecules. *J.*
27
28 *Chem. Phys.* **2002**, *117*(3), 1098– 1102.

29
30
31 (20) Falcinelli, S., Vecchiocattivi, F., Alagia, M., Schio, L., Richter, R., Stranges, S., Catone, D.,
32
33 Arruda, M. S., Mendes, L. A. V., Palazzetti, F., Aquilanti, V., Pirani, F. Double photoionization
34
35 of propylene oxide: A coincidence study of the ejection of a pair of valence-shell electrons. *J.*
36
37 *Chem. Phys.* **2018**, *148*, 114302.

38
39
40 (21) Falcinelli, S., Rosi, M., Vecchiocattivi, F., Pirani, F., Alagia, M., Schio, L., Richter, R.,
41
42 Stranges, S. Double photoionization of simple molecules of astrochemical interest. *ICCSA* **2018**,
43
44 *LNCS 10961*, 746-762.

- 1
2
3 (22) Falcinelli, S., Candori, P., Pirani, F., Vecchiocattivi, F. The role of the charge transfer in
4 stability and reactivity of chemical systems from experimental findings. *Phys. Chem. Chem.*
5
6 *Phys.* **2017**, *19(10)*, 6933–6944.
7
8
9
10
11 (23) Salén, P., Yatsyna, V., Schio, L., Feifel, R., Richter, R., Alagia, M., Stranges, S.,
12
13 Zhaunerchyk, V. NEXAFS spectroscopy and site-specific fragmentation of *N*-methylformamide,
14
15 *N,N*-dimethylformamide, and *N,N*-dimethylacetamide. *J. Chem. Phys.* **2016**, *144*, 244310.
16
17
18
19 (24) Pei, L., Carrascosa, E., Yang, N., Falcinelli, S., Farrar, J. M. Velocity Map Imaging Study
20
21 of Charge-Transfer and Proton-Transfer Reactions of CH₃ Radicals with H₃⁺. *J. Phys. Chem.*
22
23 *Lett.* **2015**, *6(9)*, 1684–1689.
24
25
26
27 (25) Alagia, M., Candori, P., Falcinelli, S., Lavollée, M., Pirani, F., Richter, R., Stranges, S.,
28
29 Vecchiocattivi, F. Double photoionization of N₂O molecules in the 28-40 eV energy range.
30
31 *Chem. Phys. Lett.* **2006**, *432*, 398-402.
32
33
34
35 (26) Alagia, M., Candori, P., Falcinelli, S., Lavollée, M., Pirani, F., Richter, R., Stranges, S.,
36
37 Vecchiocattivi, F. Double Photoionization of CO₂ molecules in the 34-50 eV Energy range. *J.*
38
39 *Phys. Chem. A* **2009**, *113*, 14755-14759.
40
41
42
43 (27) Alagia, M., Candori, P., Falcinelli, S., Lavollée, M., Pirani, F., Richter, R., Stranges, S.,
44
45 Vecchiocattivi, F. Dissociative double photoionization of CO₂ molecules in the 36–49 eV energy
46
47 range: angular and energy distribution of ion products. *Phys. Chem. Chem. Phys.* **2010**, *12*, 5389-
48
49 5395.
50
51
52
53
54
55
56
57
58
59
60

1
2
3 (28) Alagia, M., Candori, P., Falcinelli, S., Pirani, F., Pedrosa Mundim, M. S., Richter, R., Rosi,
4 M., Stranges, S., Vecchiocattivi, F. Dissociative double photoionization of benzene molecules in
5 the 26–33 eV energy range. *Phys. Chem. Chem. Phys.* **2011**, *13*, 8245-8250.
6
7

8
9
10 (29) Alagia, M., Candori, P., Falcinelli, S., Pirani, F., Mundim, M. S. P., Richter, R., Rosi, M.,
11 Stranges, S., Vecchiocattivi, F. Dissociative double photoionization of singly deuterated benzene
12 molecules in the 26–33 eV energy range. *J. Chem. Phys.* **2011**, *135*, 144304.
13
14
15

16 (30) Alagia, M., Callegari, C., Candori, P., Falcinelli, S., Pirani, F., Richter, R., Stranges, S.,
17 Vecchiocattivi, F. Angular and energy distribution of fragment ions in dissociative double
18 photoionization of acetylene molecules at 39 eV. *J. Chem. Phys.* **2012**, *136*, 204302.
19
20
21

22 (31) Falcinelli, S., Alagia, M., Farrar, J. M., Kalogerakis, K. S., Pirani, F., Richter, R., Schio, L.,
23 Stranges, S., Rosi, M., Vecchiocattivi, F. Angular and energy distributions of fragment ions in
24 dissociative double photoionization of acetylene molecules in the 31.9-50.0 eV photon energy
25 range. *J. Chem. Phys.* **2016**, *145*, 114308.
26
27
28

29 (32) Lavollée, M. A new detector for measuring three-dimensional momenta of charged particles
30 in coincidence. *Rev. Sci. Instrum.* **1990**, *70*, 2968-3974.
31
32
33

34 (33) Lundqvist, M., Baltzer, P., Edvardsson, D., Karlsson, L., Wannberg, B. Novel Time of
35 Flight Instrument for Doppler Free Kinetic Energy Release Spectroscopy. *Phys. Rev. Lett.* **1995**,
36 *75*, 1058-1061.
37
38
39

40 (34) Field, T.A., Eland, J.H.D. Lifetimes of metastable molecular doubly charged ions. *Chem.*
41 *Phys. Lett.* **1993**, *211*, 436-442.
42
43
44
45
46
47
48
49
50
51
52
53
54
55
56
57
58
59
60

1
2
3 (35) Alagia, M., Bodo, E., Decleva, P., Falcinelli, S., Ponzi, A., Richter, R., Stranges, S. The soft
4 X-ray absorption spectrum of the allyl free radical. *Phys. Chem. Chem. Phys.* **2013**, *15*(4), 1310-
5 1318.
6
7

8
9
10 (36) Alagia, M., Candori, P., Falcinelli, S., Mundim, K. C., Mundim, M. S. P., Pirani, F., Richter,
11 M., Stranges, S., Vecchiocattivi, F. Lifetime and kinetic energy release of metastable dications
12 dissociation. *Chem. Phys.* **2012**, *398*, 134-141.
13
14
15

16
17 (37) Falcinelli, S., Rosi, M., Cavalli, S., Pirani, F., Vecchiocattivi, F. Stereoselectivity in
18 Autoionization Reactions of Hydrogenated Molecules by Metastable Noble Gas Atoms: The
19 Role of Electronic Couplings. *Chemistry Eur. J.* **2016**, *22*(35), 12518-12526.
20
21
22

23
24 (38) Falcinelli, S., Vecchiocattivi, F., Pirani, F. Adiabatic and nonadiabatic effects in the
25 transition states of state to state autoionization processes. *Phys. Rev. Lett.* **2018**, *121*(16), 163403.
26
27
28

29
30 (39) Falcinelli, S., Bartocci, A., Cavalli, S., Pirani, F., Vecchiocattivi, F. Stereo-dynamics in
31 collisional autoionization of water, ammonia, and hydrogen sulfide with metastable rare gas
32 atoms: competition between intermolecular halogen and hydrogen bonds. *Chemistry Eur. J.*
33 **2016**, *22*(2), 764-771.
34
35
36
37

38
39 (40) Zare, R. N., and Herschbach, D. R. Angular Distribution of Products in Molecular
40 Photodissociation. *Bull. Am. Phys. Soc.* **1962**, *7*, 458.
41
42
43

44
45 (41) Zare, R. N. Photoejection Dynamics. *Mol. Photochem.* **1972**, *4*, 1-37.
46
47
48

49
50 (42) Ashfold, M. N. R., Hendrik Nahler, N., Orr-Ewing, A. J., Vieuxmaire, O. P. J., Toomes, R.
51 L., Kitsopoulos, T. N., et al. Imaging the dynamics of gas phase reactions. *Phys. Chem. Chem.*
52 *Phys.* **2006**, *8*, 26-53.
53
54
55
56

1
2
3 (43) Nobes, R. H., Bouma, W. J., and Radom, L. Structures and Stabilities of Gas-Phase $C_2H_3O^+$
4 Ions: An ab Initio Molecular Orbital Study. *J. Am. Chem. Soc.* **1983**, *105*, 309-314.
5
6

7
8 (44) Burgers, P. C., Holmes, J. L., Szulejko, J. E., Mommers, A. A., Terlouw, J. K. The gas phase
9 ion chemistry of the acetyl cation and isomeric $[C_2H_3O]^+$ ions. On the structure of the $[C_2H_3O]^+$
10 daughter ions generated from the enol of acetone radical cation. *J. Mass Spectrom.* **1983**, *18*, 254-
11 262.
12
13
14
15
16

17
18 (45) Becke, A. D. Density-functional thermochemistry. III. The role of exact exchange. *J. Chem.*
19 *Phys.* 1993, *98*, 5648-5652.
20
21
22

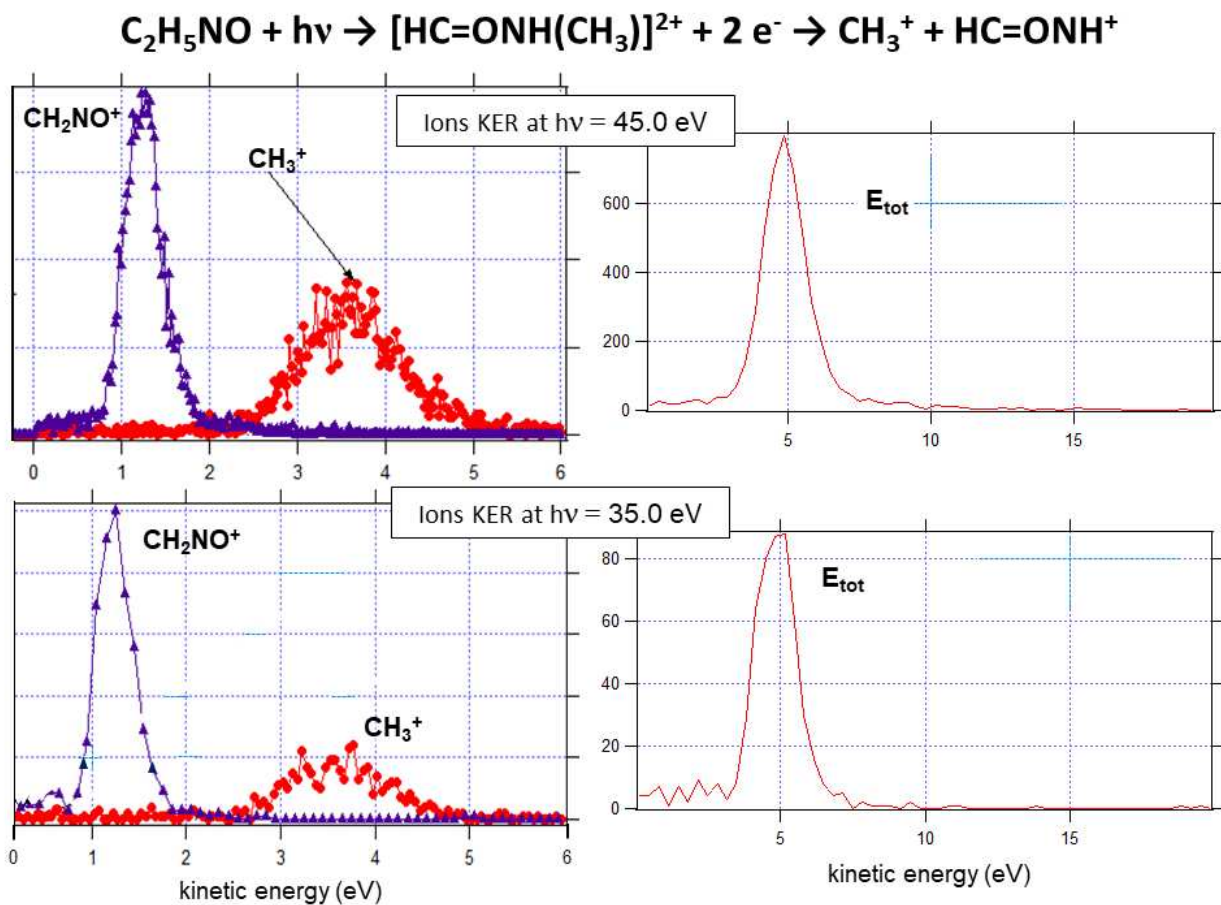
23
24 (46) Stephens, P. J., Devlin, F. J., Chabalowski, C. F., and Frisch, M. J. Ab Initio Calculation of
25 Vibrational Absorption and Circular Dichroism Spectra Using Density Functional Force Fields. *J.*
26 *Phys. Chem.* 1994, *98*, 11623-11627.
27
28
29

30
31 (47) Lin, Y.-S., Tsai, C.-C., Lin, H.-R., Hsieh, T.-L., Chen, J.-L., Hu, W.-P., Ni, C.-K., Liu, C.-L.
32 Highly Selective Dissociation of a Peptide Bond Following Excitation of Core Electrons. *J. Phys.*
33 *Chem. A* **2015**, *119*, 6195-6202.
34
35
36
37

38
39 (48) Li, Z., Dawley, M. M., Carmichael, I., Ptasińska, S. Electron-Induced Fragmentation of
40 Methylated Formamides. *Int. J. Mass Spectrom.* **2016**, *410*, 36-46.
41
42
43

44 (49) Adande, G. R., Woolf, N. J., Ziurys, L. M. Observations of Interstellar Formamide:
45 Availability of a Prebiotic Precursor in the Galactic Habitable Zone. *Astrobiology* **2013**, *13*(5),
46 439-453.
47
48
49
50
51
52
53
54
55
56
57
58
59
60

For TOC Only



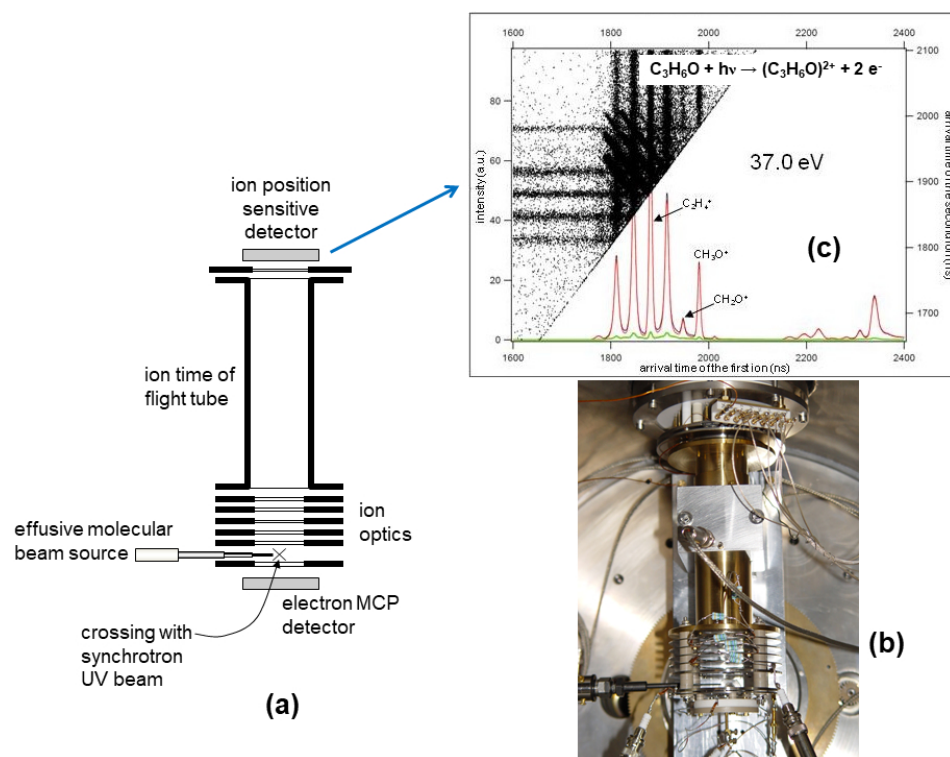


Figure 1

254x190mm (96 x 96 DPI)

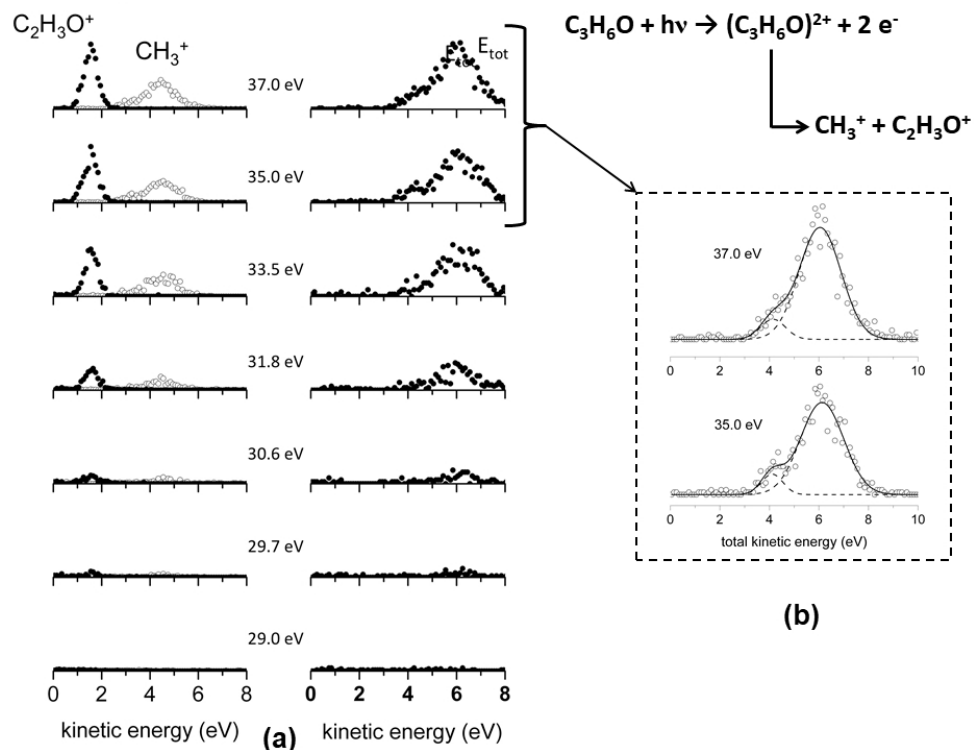
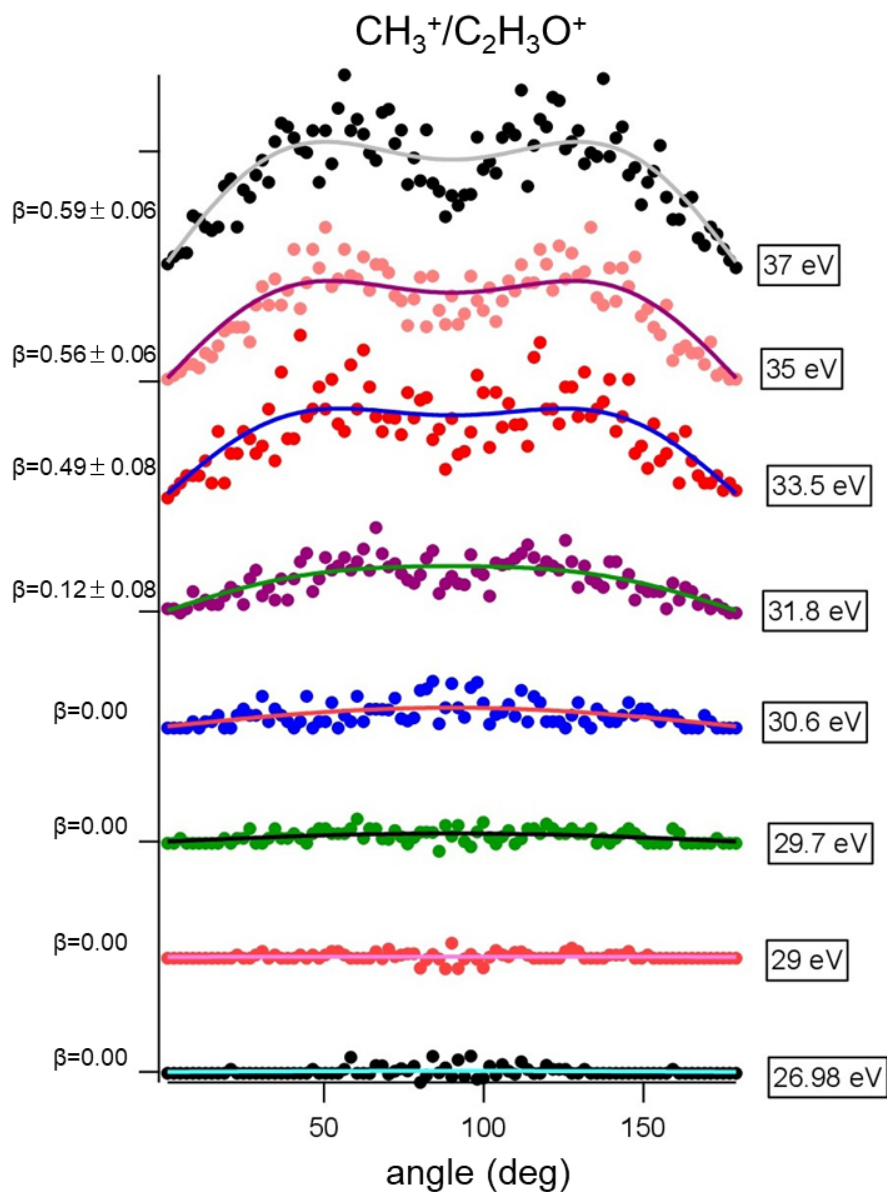


Figure 2

254x190mm (96 x 96 DPI)



45 Figure 3. Recorded angular distributions of $\text{CH}_3^+/\text{C}_2\text{H}_3\text{O}^+$ fragment ion pair products formed by Coulomb
46 explosion of the $\text{C}_3\text{H}_6\text{O}_2^+$ dication at different photon energies. In the ordinate axis dots intensity are in
47 arbitrary units. For clarity the error bars are omitted since they are of the same order of magnitude of the
48 dot dimensions. On the left side are reported the calculated anisotropy parameters β using equation (2) for
49 each collected angular distribution (see text).

50 190x254mm (96 x 96 DPI)

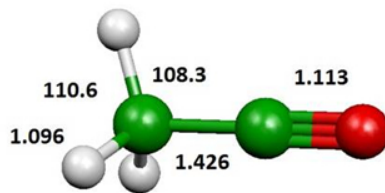
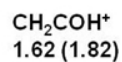
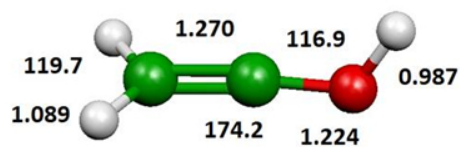
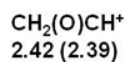
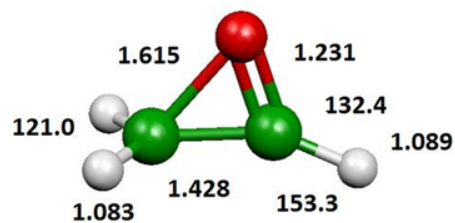


Figure 4. B3LYP optimized geometries (\AA , and $^\circ$) of the three stable $\text{C}_2\text{H}_3\text{O}^+$ isomers; relative energies (eV) computed at B3LYP (CCSD(T)) level have been reported (see text).

190x254mm (96 x 96 DPI)

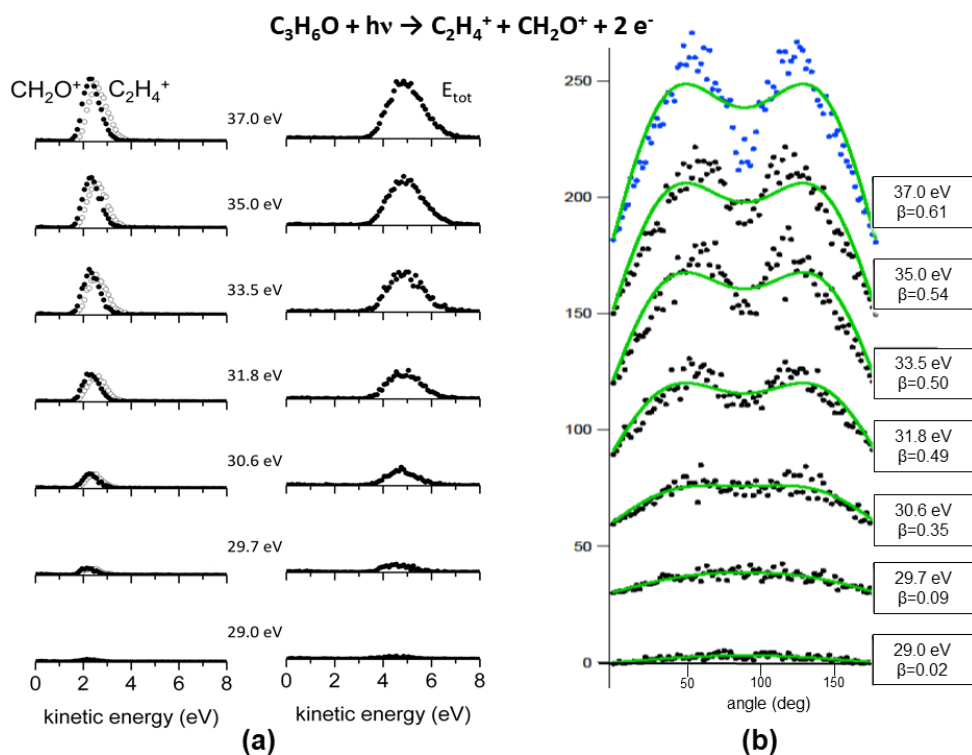


Figure 5. a) The kinetic energy released (KER) distributions for the $\text{C}_2\text{H}_4^+/\text{CH}_2\text{O}^+$ ion pair products generated in the two-body fragmentation process following the double photoionization experiment of propylene oxide as a function of the photon energy: the left panel shown KERs for each single product ion, while in right panel total ion KER distributions are reported; (b) Angular distributions of $\text{C}_2\text{H}_4^+/\text{CH}_2\text{O}^+$ fragment ion pair products formed by Coulomb explosion of the $\text{C}_3\text{H}_6\text{O}_2^+$ dication at different photon energies. In the ordinate axis dots intensity are in arbitrary units. For clarity the error bars are omitted since they are of the same order of magnitude of the dot dimensions. On the right side are reported the calculated anisotropy parameters β using equation (2) for each collected angular distribution (see text).

254x190mm (96 x 96 DPI)

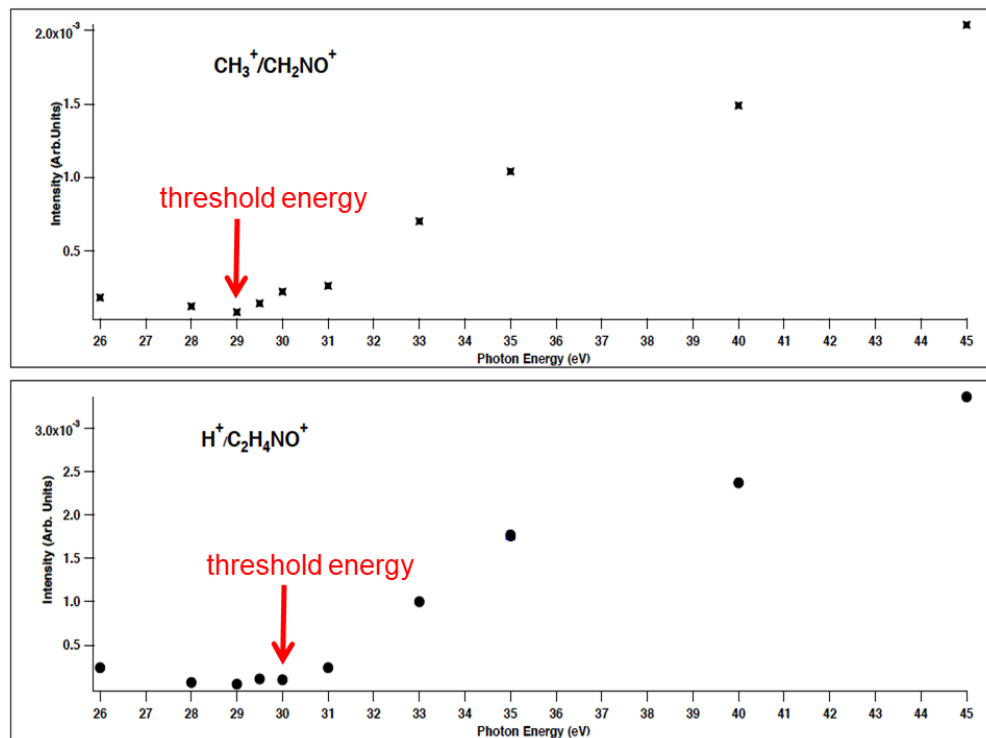


Figure 6. The relative cross sections as function of the investigated photon energy as obtained in the double photoionization experiment of N-methylformamide in the 26-45 eV photon energy range.

254x190mm (96 x 96 DPI)

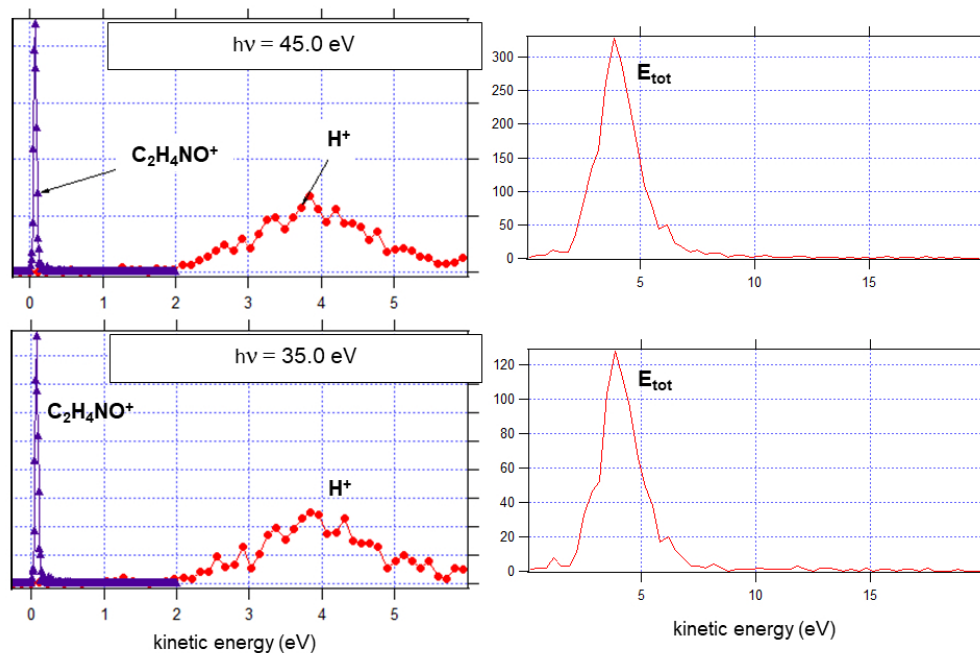
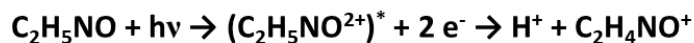


Figure 7. The kinetic energy released (KER) distributions for the $\text{H}^+/\text{C}_2\text{H}_4\text{NO}^+$ ion pair products generated in the two-body fragmentation process following the double photoionization experiment of N-methylformamide at two different photon energies (35.0 eV - lower panel and 45.0 eV - upper panel): the pictures on the left side show KERs for each single product ion, while on the right side total ion KER distributions are reported.

254x190mm (96 x 96 DPI)

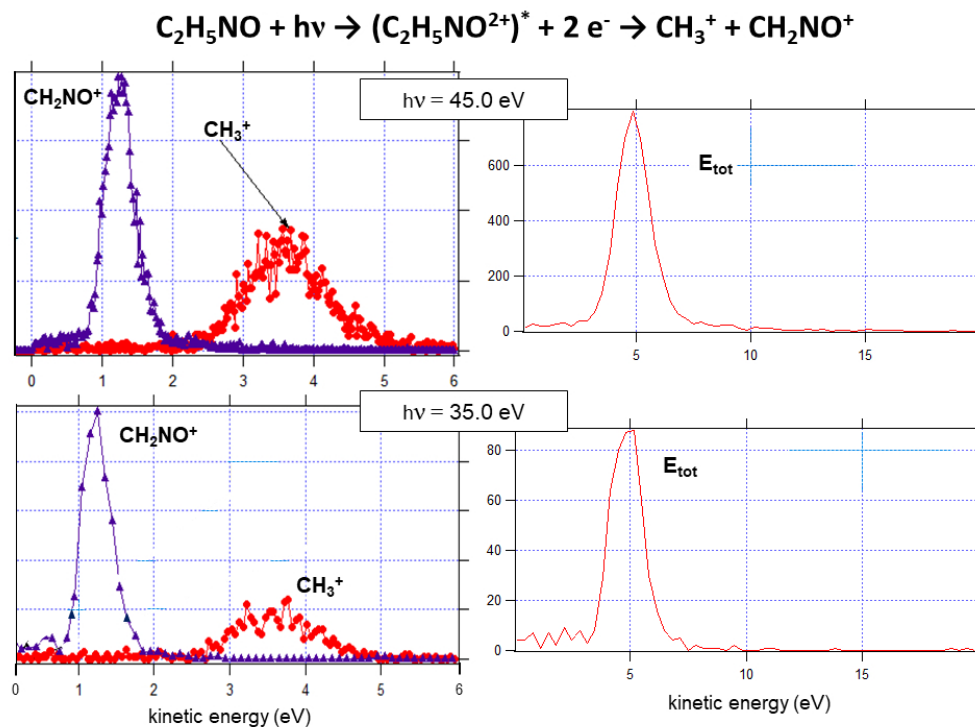


Figure 8. The kinetic energy released (KER) distributions for the $\text{CH}_3^+/\text{CH}_2\text{NO}^+$ ion pair products generated in the two-body fragmentation process following the double photoionization experiment of N-methylformamide at two different photon energies (35.0 eV - lower panel and 45.0 eV - upper panel): the pictures on the left side show KERs for each single product ion, while on the right side total ion KER distributions are reported.

254x190mm (96 x 96 DPI)